

Project Miura

Final Science Report

Colorado Space Grant Consortium

Nicholas Bearns, Dawson Beatty, Rhett Crismon, Adam Farmer, Sean Fearon,
Jacob Jeffries, Courtney Kelsey, Brendan Lutes, Anastasia Muszynski,
Alexandra Paquin, Andrew Pfefer, Mary Rahjes, Melanie Smith, Lucas Zardini,
Micah Zhang

December 8, 2017



Contents

1	Mission Premise	1
1.1	Background	1
1.2	Mission Statement	1
1.3	Mission Objectives	1
1.4	Context	2
1.5	Concept of Operations	2
2	Design	3
2.1	Design Overview	3
2.2	Payload	6
2.2.1	Origami Folding Design	6
2.2.2	Material Design	7
2.2.3	Integration With Payload	8
2.2.4	Deployment Mechanism	9
2.3	Structures	9
2.3.1	Lower Housing	9
2.3.2	Camera Support Structure and Cameras	10
2.4	Flight Software	11
2.4.1	Overview	11
2.4.2	Design	11
2.4.3	Uplink Commands	12
2.4.4	Downlink Packets	14
2.5	Electrical and Power Systems	15
2.5.1	HASP Integration	15
2.5.2	Power Budget	15
2.5.3	PCB Design	15
2.5.4	Wire Management	16
3	Testing	17
3.1	Payload Testing	17
3.1.1	Tensile Testing	17
3.1.2	Outgassing Testing	17
3.1.3	Optical Testing	17
3.1.4	Thermal Testing	18
3.2	Systems Testing	19
3.3	Integration Testing	19
4	Flight Overview	20
4.1	Timeline	20
5	Results and Analysis	22
5.1	Environmental Results	22
5.2	Root Cause Analysis	24
5.2.1	Initial Possible Causes	24
5.2.2	Motor Driver Test	26
5.2.3	Failure Analysis	26
5.3	Extension Cycles	27
5.4	Material Analysis	27
5.4.1	Post-Flight Visual Inspection	27
5.4.2	Post-Flight Magnified Inspection	28
5.5	Thermal Behavior	31
5.6	Design Analysis	32
5.6.1	Origami Design	32
5.6.2	Packing Ratio	32
5.7	Material Accommodation to Design	33

6 Conclusions	34
6.1 Mission Objectives	34
6.2 Minimum Success Criteria	34
6.3 Requirements	34
6.4 Overall System Functionality	35
7 Lessons Learned and Recommendations	36
7.1 Payload	36
7.2 Structures	36
7.3 Flight Software	36
7.4 Electrical and Power Systems	37
8 Moving Forward	38
8.1 Miura II Recommendations	38
9 Acknowledgments	38
A Publications	40
B Team Demographics	40
C HASP Longitudinal Tracking	40
D Requirements	41
E Code Functional Block Diagram	43

Abstract

Project Miura seeks to apply the existing technique of Miura Origami to the structural layer of a reusable soft-shell structure for space flight. Key engineering objectives included manufacturing of a space-grade deployable structure resistant to tears and inversions in nominal use case. Mission included analysis of system performance in near-space environment, emphasizing material response to temperature change. Near-space testing environment provided by the High Altitude Student Platform (HASP) via a 14-hour launch in September 2017. Payload experienced a motor failure three hours into flight and was unable to complete desired number of test expansions. Fortunately, limited flight data as well as results from Temperature and VACuum (TVAC) chamber tests still suffice to verify this method as a structural layer for future missions.

1 Mission Premise

1.1 Background

Current expandable soft-shell structures tend to be single use, and are not capable of folding back into the organized and space-efficient form in which they were initially launched. This could be made possible by folding the structure using an origami technique called Miura Origami. Similar techniques could be adapted for cost-efficient spacecraft habitats or antennas, and could prove instrumental with the demand for human activity on Mars.

Deployable structures saw an increase in use with the launch of Bigelow Aerospace's Expandable Activity Module (Fig. 1) which was launched to the International Space Station in April of 2016. The BEAM and other modules like it have no way to repack into the space-efficient form in which they were originally launched.

Japanese Astrophysicist Koryo Miura invented a tessellating origami pattern (Fig. 2) which now bears his name. This style of folding allows for transition between a large and small surface area by applying a force along a single axis.

Project Miura seeks to apply this technique of origami to a space grade material in construction of a reusable soft-shell structure. To show the feasibility of this system in a near-space environment, the structure was launched on the High Altitude Student Platform (HASP) launch vehicle. This mission focuses on implementing an origami folding design to the structural layer of a small module as a proof of concept, characterizing performance of the structural layer in the near space environment, and laying groundwork for additional layers in possible subsequent missions.

1.2 Mission Statement

Project Miura will controllably extend, sustain, and retract a soft shell structure multiple times on the High Altitude Student Platform while recording and monitoring the process to assess the viability of reusable collapsible structures for space flight.

1.3 Mission Objectives

Mission Objectives:

1. Use a mechanical system to extend, sustain, and retract the soft shell structure.
2. Quantitatively monitor the extension, retention, and retraction of the soft shell structure.
3. Record high resolution video to analyze the soft shell structure's deployment process, retention of the extended state, and retraction into a compact form.



Figure 1: Deployed Bigelow Aerospace Expandable Activity Module (BEAM) attached to the International Space Station. *Courtesy: nasa.gov*

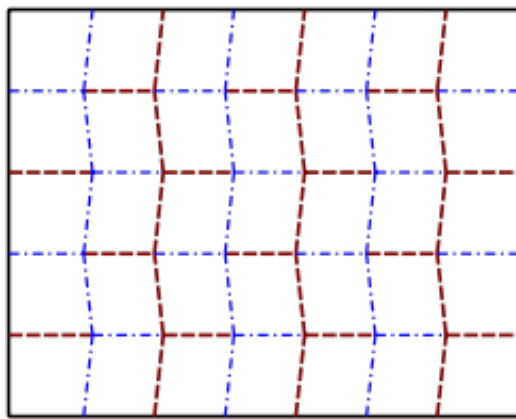


Figure 2: Example folding pattern of Miura origami

1.4 Context

One of the first concepts for an inflatable space station appeared in 1961 as a concept produced by Goodyear. Throughout the successive decades, the idea of deployable habitats was occasionally brought up in different conceptual contexts. NASA designed an inflatable module for the International Space Station in 1997 as a replacement for the rigid habitation module on the station, which was called TransHab (Transit Habitat). Following an order from Congress in 2000, NASA was disallowed from continuing the development of TransHab, and the private corporation Bigelow Aerospace purchased the patent rights to continue developing the concept. Bigelow's first modules were Genesis I and Genesis II, which were investigatory payloads of the viability of expandable modules. Bigelow's latest expandable habitat is the BEAM (Bigelow Expandable Activity Module), which docked to the International Space Station and pressurized in April and May 2016.

Deployable habitats possess significant advantages over their solid counterparts when it comes to human spaceflight. Deployable habitats can be designed to be more resistant to debris impact, more radiation-proof, are typically lighter, and can be designed to be larger on orbit than their rigid counterparts, by virtue of their soft-bodied design. The greatest attributes of soft bodied habitats lie in this ability to be deformed into compact profile, which can be more efficiently stacked upon a launch vehicle, and manipulated in space. One of the greatest drawbacks of current deployable structure technology is that the processes utilized for deployment, inflation via pressurization, cannot be effectively utilized for stowing the module. This means that once one of these structures is deployed on orbit, it is in its final state: at this point, it is as cumbersome to manipulate in space as a rigid structure. Project Miura will develop and test the folding mechanism necessary to create a deployable structure that can be retracted and stowed away for efficient secondary transportation. Such technology may prove instrumental in future human exploration missions.

1.5 Concept of Operations

The Concept of Operations for project Miura is given in Figure 3 which outlines the extension-contraction cycles which are repeated indefinitely throughout the mission. Figure 4 is the higher level, system wide Principle of Operations. It outlines the entire mission from launch to recovery. This schedule was followed for the actual flight.

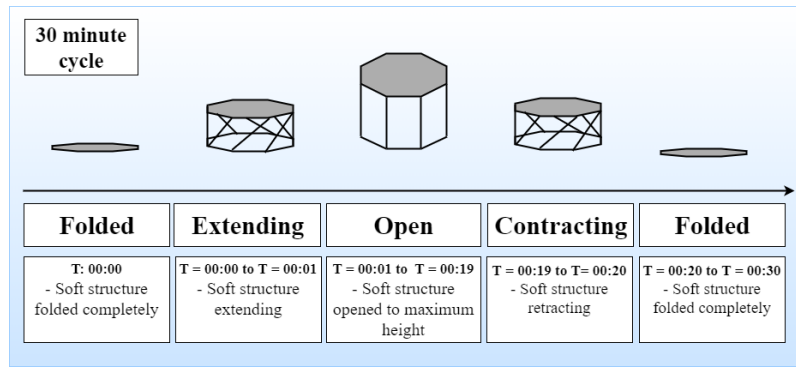


Figure 3: Concept of Operations

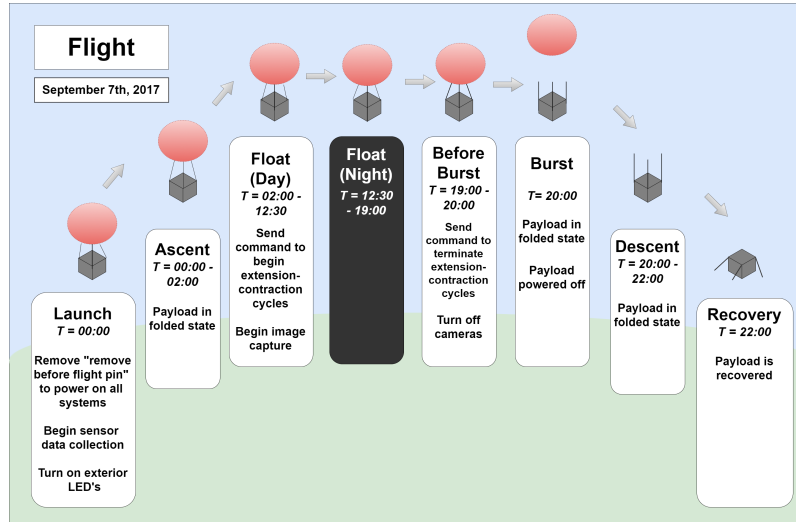


Figure 4: Principle of Operations

2 Design

2.1 Design Overview

Miura has five main systems shown in Figure 5. The Command and Data Handling (CDH) system primarily consists of Raspberry Pi, and communicates to HASP via a DB9 cord over an RS-232 communication protocol. The Electronics and Power System (EPS) receives 30 VDC from an EDAC connector and provides 5 VDC to all of the other systems. The CDH system coordinates all of the other systems and communicates with the team on the ground. Sensors all around the payload to keep track of temperature and other information of interest.

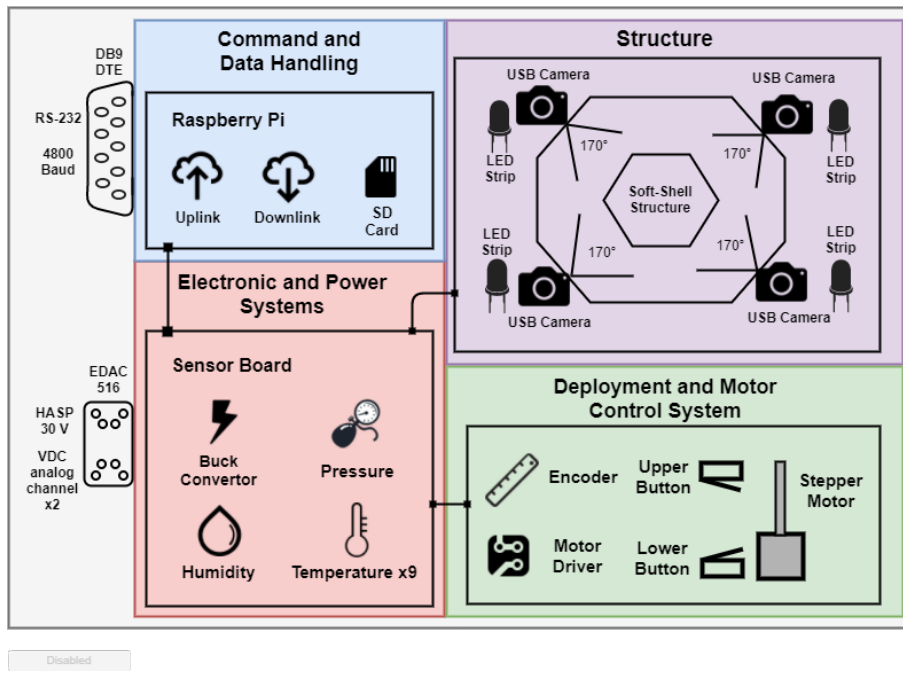


Figure 5: Systems Functional Block Diagram

As shown in Figures 6, 7, and 15, the major components on Miura are the Kevlar-Epoxy extendable, the deployment mechanism, the cameras, and the various EPS components located in the base. The deployment mechanism employs use of a stepper motor, screw drive, bearings, and support rods to allow the extension of the soft-shell in the vertical direction while still allowing free angular rotation of the payload. The cameras are used to characterize performance of the payload throughout flight. The EPS components are used to control a variety of functions including power distribution, motor function, camera activation, and serial communications.

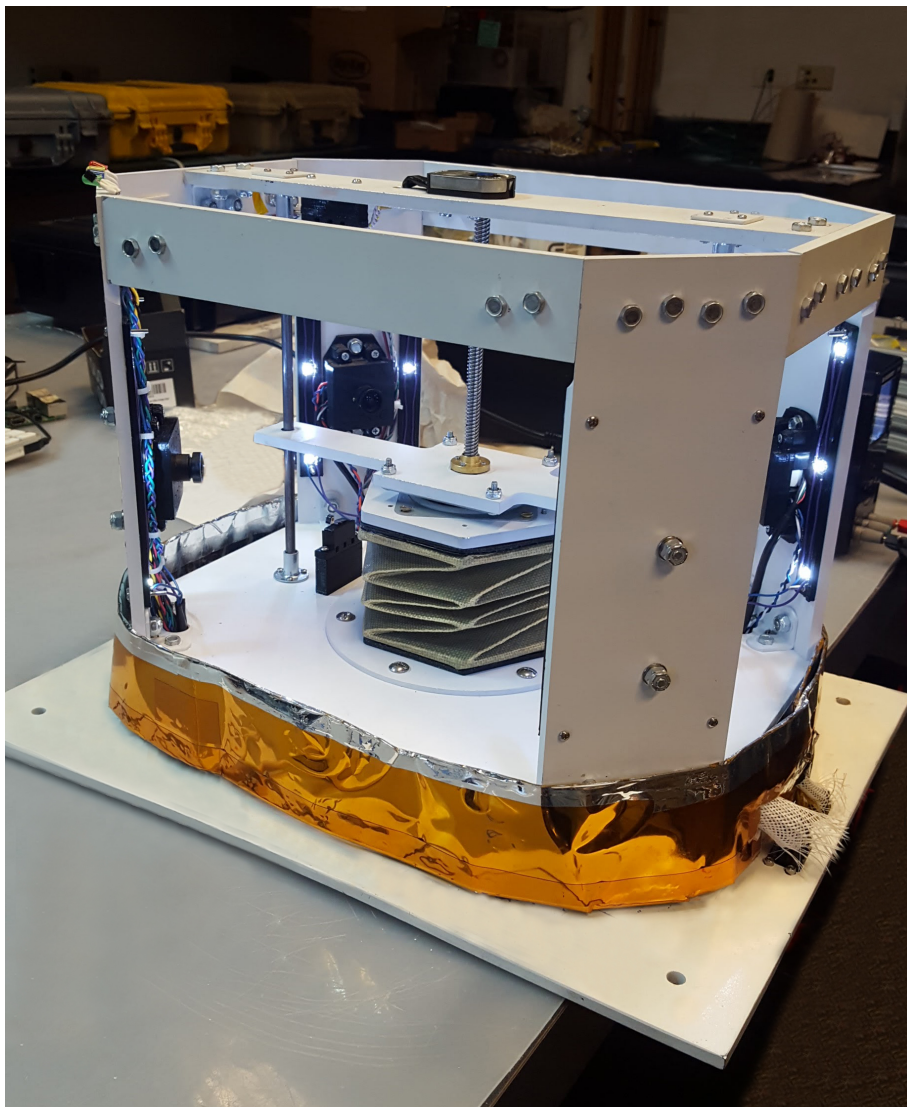


Figure 6: Picture of Miura payload

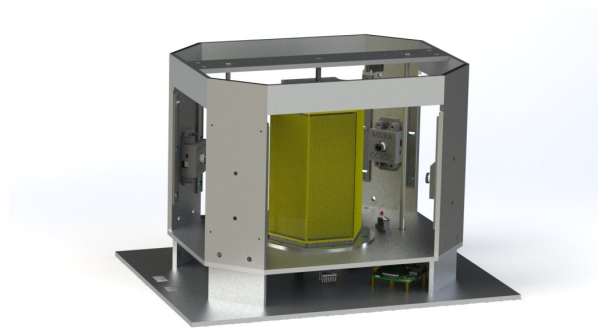


Figure 7: Render of overall payload

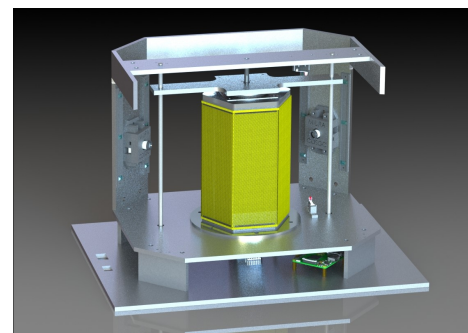


Figure 8: Major components of Miura

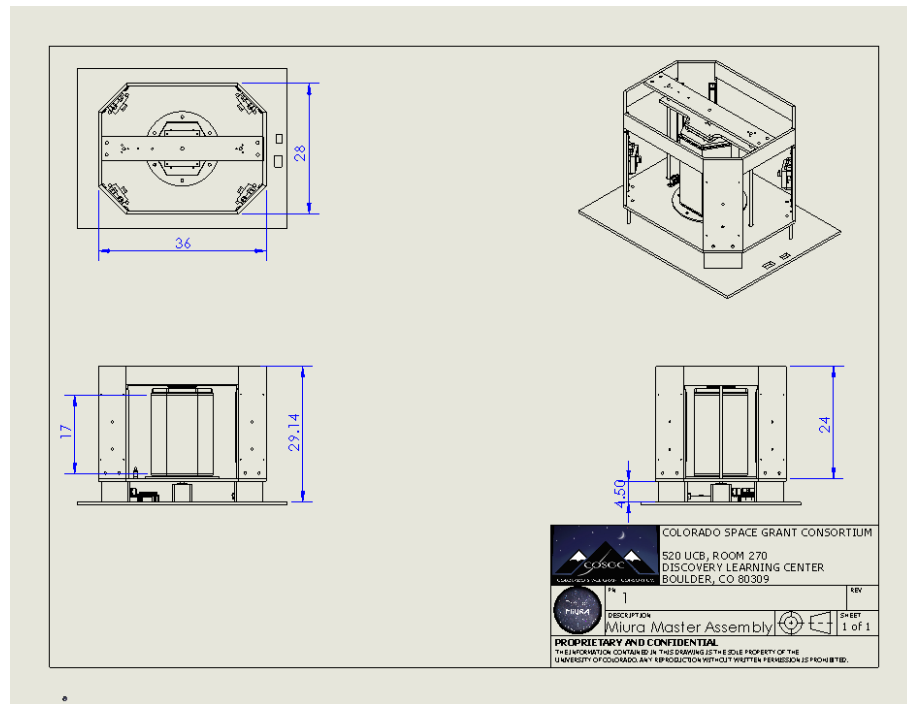


Figure 9: Dimensioned Drawing of Miura

2.2 Payload

The role of the payload subteam is to design and fabricate the soft-shell structure (hereafter referred to as 'model') and deployment mechanism. This role includes all research and analysis of the materials and folding design of the model, as well as environmental sensor and camera placement and post-flight analysis.

2.2.1 Origami Folding Design

The folding technique utilized is based upon Miura origami, for which this project is named. Miura origami involves tessellated patterns of triangles and parallelograms. This type of design allows for the transformation of a nearly two dimensional object to a three dimensional object, with a force applied on only one axis. The technique was developed from basic origami techniques by Koryo Miura and Masamori Sakamaki from Tokyo University's Institute of Space and Aeronautical Science to improve the folding techniques of solar panels^[2]. The basic design is called the Miura-Ori map (Fig. 2), and uses a parallelogram pattern^[2]. The pattern utilizes alternating mountain folds and valley folds, which makes it strong, less prone to tearing and fold inversion, and ensures it collapses into the same shape each time. In addition to being extraordinarily strong, resistant to distortion, and collapsible, the map will fully extend in all directions when pulled along only one axis. Though this technique has been used to created deployment mechanisms for solar panels, it has never before been applied to a soft-sided structure of the habitat variety.

When developing the design for the payload, reusability, stowability, and reliability were emphasized. This lead to selecting a design that would provide a high stowed volume to expandable volume ratio, would have a low risk of developing fold inversions, and would have a low risk of tearing the material.

The origami design developed for the module flown on project Miura was based upon the Kresling fold (helically triangulated cylinder), which modifies the Miura-Ori map design to collapse into a hexagon (Fig. 10). This origami design features two regimes, a rigid regime and regime of deformation. During the rigid regime (0 - 74% extension), all planar regions remain flat and no deformations of fold occur. During the regime of deformation (74 - 100% extension), valley folds (concave folds) deform and "puff" outwards to accommodate the full extension of the structure, and planar regions curve slightly to accommodate a more cylindrical shape.

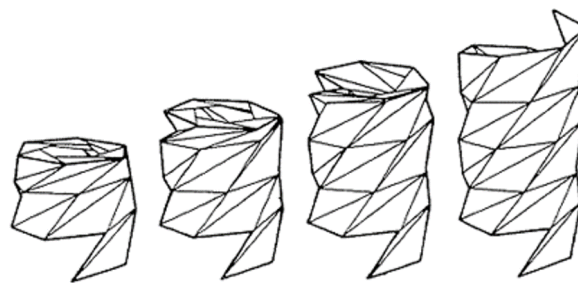


Figure 10: Extension of Kresling Fold (Helically Triangulated Cylinder)

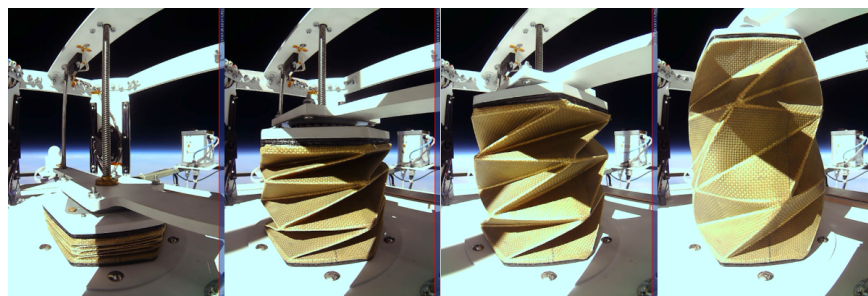


Figure 11: Extension of Miura Model During Flight

The design involves a 90 degree rotation of the top face from fully collapsed to fully extended. Because of the geometry of the Miura folds, only force needed to expand the structure is in the positive z-axis direction. As long as the top face can rotate freely, the structure will fully expand. The rotational aspect creates a stable expansion in the positive z-axis direction, and mitigates the risks of fold inversions. The twisting motion did however put additional stress and strain on the material.

2.2.2 Material Design

Since the folding design was to be implemented in a structural layer, Kevlar was chosen as the base material, as it is currently used as a structural component of soft space structures such as space suits and the Bigelow Beam module. When selecting the specific types of materials to be used, prevention of tear and hole formation, and the ability of the material to implement design were considered. The final materials selected for the structural layer of the module were a 1140 denier Kevlar 49 plain weave, with a coating of 2216 Scotch Weld 2 part epoxy adhesive. A single layer of epoxied Kevlar was used to allow unobstructed monitoring of the entire structure throughout the flight, and thus understand the material's behavior in different environmental conditions prior to adding any additional layers.

The desired folding behavior was achieved through the strategic placement of epoxy on a flat net of the folding design (Fig. 12). Epoxy both stiffens the Kevlar, as well as secures the individual strands of Kevlar in place. Two layers of epoxy were applied to the planar regions of the design, one on each side of the material (Fig. 13). All diagonal creases were left un-epoxied to preserve the flexibility of the material. Lines of epoxy 1.5 mm wide were applied to all horizontal creases on the interior of the fabric to increase stability during extension and retraction. Parallelogram-shaped regions of epoxy (Fig. 14) were added to the interior of the fabric on the vertices to hold the individual fibers in place and prevent shifting of fibers during extension/ retraction. Four coats of epoxy were applied in total to the flat sheet of Kevlar. The epoxy was cured by baking the material for 2 hours in an oven at 65 °C after the application of each layer.

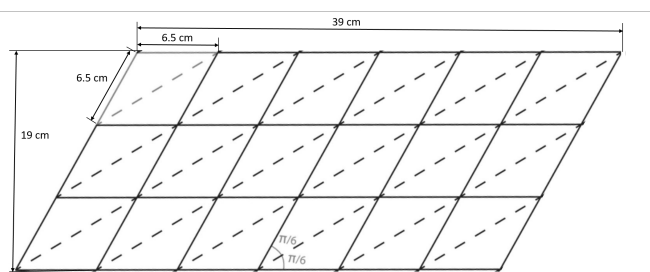


Figure 12: Net of Kresling Fold as applied to material

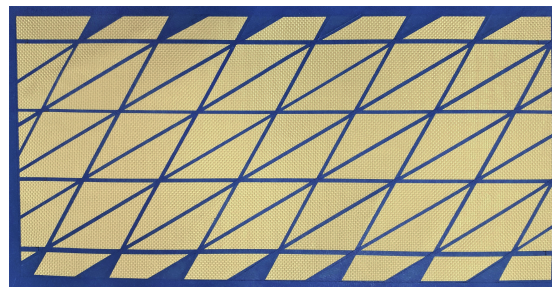


Figure 13: Kevlar material with net applied, prepped for first coat of epoxy. Epoxy is applied to all exposed Kevlar.



Figure 14: Epoxy pattern at the vertex on interior face of the Model. The parallelogram shape prevents the shifting of Kevlar strands. The horizontal epoxy line improves dimensional stability of the crease during expansion. Epoxy is more gray in color, while plain, exposed Kevlar is yellow in appearance

2.2.3 Integration With Payload

To attach the soft material to the structure and deployment mechanism, two sets of integration plates were fabricated. These plates were 3-D printed, two on each base with one on the interior and one on the exterior and the epoxied Kevlar sandwiched between them. The flat sheet of Kevlar was overlapped 2.5 cm, and the seam epoxied to create a cylindrical shell. The top and bottom edges of the material were then epoxied in place between the integration plates and secured with bolts. Each set of integration plates was then bolted to an aluminum plate, which was bolted to the platform. No pre-creasing of the module was required, as the material naturally bent at the designated creases once the integration plates were added. The finished, folded material is shown in Figure 15, and the layout of the integrated model is shown in Figure 16.



Figure 15: Origami Shell of Expandable

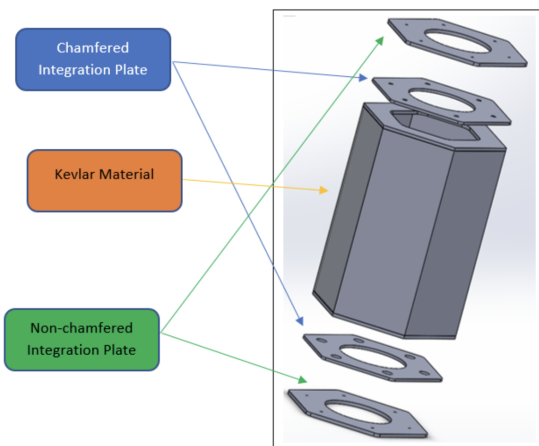


Figure 16: Exploded View of the Expandable

2.2.4 Deployment Mechanism

The deployment mechanism that enables the extension of the model consists of six main components. These are the stepper motor, screw drive, guide rods, integration plates, rotation mechanism, and the support bar. As previously mentioned, the stepper motor is connected directly to the HASP provided base plate. A screw drive is connected directly to the motor shaft. This stepper motor allows fine control of how many rotations the screw drive will undergo. This screw drive is connected to the support bar, located at the top of the payload, by an encoder. This encoder holds the screw rod in place while also keeping track of the step count produced by the motor. This support rod is connected lengthwise across the payload to the halo using the same 90 °L-brackets as the pillars used to connect to the top plate. Moving distally from the screw drive, flange mounts are found connected to the top support bar, located roughly five centimeters from the halo bars. Another set of flange mounts are attached to the top plate directly below the set on the bottom of the support bar. A steel guide rod runs between these flange mounts, keeping the payload level throughout extension and retraction.

Integration plates, machined from 6061-T6 aluminum are mounted to both the top and the bottom of the soft-shell extendable. The integration plate on the bottom is a thin aluminum ring, fixed to the top plate using six screws. This ensures the payload base stays fixed through the extension and retraction cycle. The integration plate on the top of the payload is hexagonal, fitted flush with the plastic plates comprising the ends of the payload. This top integration plate is connected to a circular ball bearing mount. This bearing allows the payload to rotate in place during its extension, a crucial component of this folding design. This bearing then connects to a horizontal bar. This horizontal bar stretches from guide rod to guide rod. On top of this horizontal bar is a carriage nut, which directly mounts to the screw drive. This horizontal bar and screw drive assembly fixes the carriage nut in place while also keeping the payload level, allowing the soft-shell structure to extend when the stepper motor is turned on. This deployment mechanism can be seen in Figure 17, pictured below.



Figure 17: Rendering of deployment mechanism, including stepper motor, guide rods, integration plates, support bar, and rotation mechanism

2.3 Structures

The role of the structures subteam is to design and fabricate a lower housing and upper support structure, as well as to provide thermal protection to all components during flight. The lower housing will contain all sensitive electrical components, ensuring that these components maintain proper thermal conditions during flight and are protected from any physical shock. This lower housing also acts as the base for the extendable payload to be mounted on. The upper support structure acts as a camera mounting surface. These cameras collect data that is crucial to payload performance characterization.

2.3.1 Lower Housing

The base plate of Miura is a half-inch thick plate of PVC, provided by HASP. The motor driver, Raspberry Pi, and PCB are all attached to the HASP base plate by standoffs. The buck converter is attached to the aluminum wall using standoffs. The buck converter was mounted to the aluminum wall to act as a heat sink, ensuring that the component does not overheat. The motor is directly connected to the base plate using four screws. Four rectangular

support columns connect the base plate to the top of the lower housing using four screws for each support columns. All wires are suspended from the top plate using wire harnesses. Holes were drilled in the top plate to allow mounting of camera support pillars, flange mounts for motor guide rods, and integration plates for the soft-shell extendable. A larger hole with a diameter of six centimeters was cut in the center, allowing the screw rod to pass through the payload and up to the top of the deployment mechanism. This assembly is shown in Figure 18

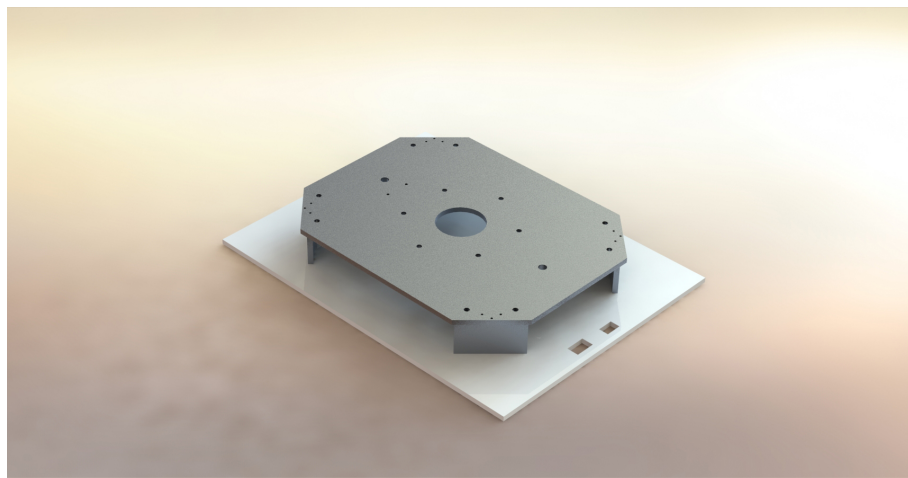


Figure 18: Rendering showing lower housing and HASP baseplate

2.3.2 Camera Support Structure and Cameras

The camera support structure consists of four large pillars and four horizontal, supporting bands connecting said pillars. The four vertical pillars will simply be referred to as “pillars” and the four horizontal supports will be referred to as the “halo” from this point on. The pillars are connected to the top plate using 90°L-brackets. The halo components are connected to the pillars using 135° custom brackets.

The purpose of the pillars is to allow mounting of LED strips and cameras. The cameras are enclosed in a 3-D printed housing, which is then bolted to the pillars. This housing serves both as a mounting platform and a protective cover for the otherwise exposed camera components. Due to the nature of the HASP flight, lighting conditions are not controlled, and can vary greatly throughout flight. The LED light strips allow a uniform brightness throughout flight resulting in the best possible images for future analysis. These LED light strips are connected to a custom 3-D printed plastic mount, which are then screwed on to the pillars. The only purpose of the halo band is to ensure that all pillars are secure through launch, flight, and landing.

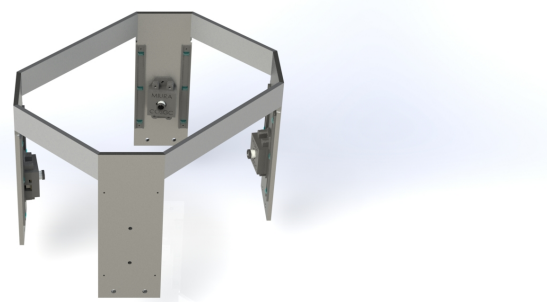


Figure 19: Rendering of camera support structure, cameras, and LED strips

2.4 Flight Software

2.4.1 Overview

The role of the flight software is to write code to tell every sensor, camera, and motor exactly what to accomplish, when to accomplish it, and how to relay the data back to the team.

A Raspberry Pi was chosen to be the payload's main computer for this project because an operating system simplifies file operations, and the Raspberry Pi allows for easy integration with sensors. All flight software was written in Python3 because of the low learning curve, and the existence of legacy code from previous missions.

To simplify the code logic and allow for simultaneous operations, the flight code relies on multithreading. The general design of the flight software employed on this payload consists of single high level "main" thread with 5 children threads. Each of the 5 children threads are specialized and are responsible for the operation of a unique function of the payload. These functions are as follows: downlink, uplink, motor command, sensor operation, and camera operation.

2.4.2 Design

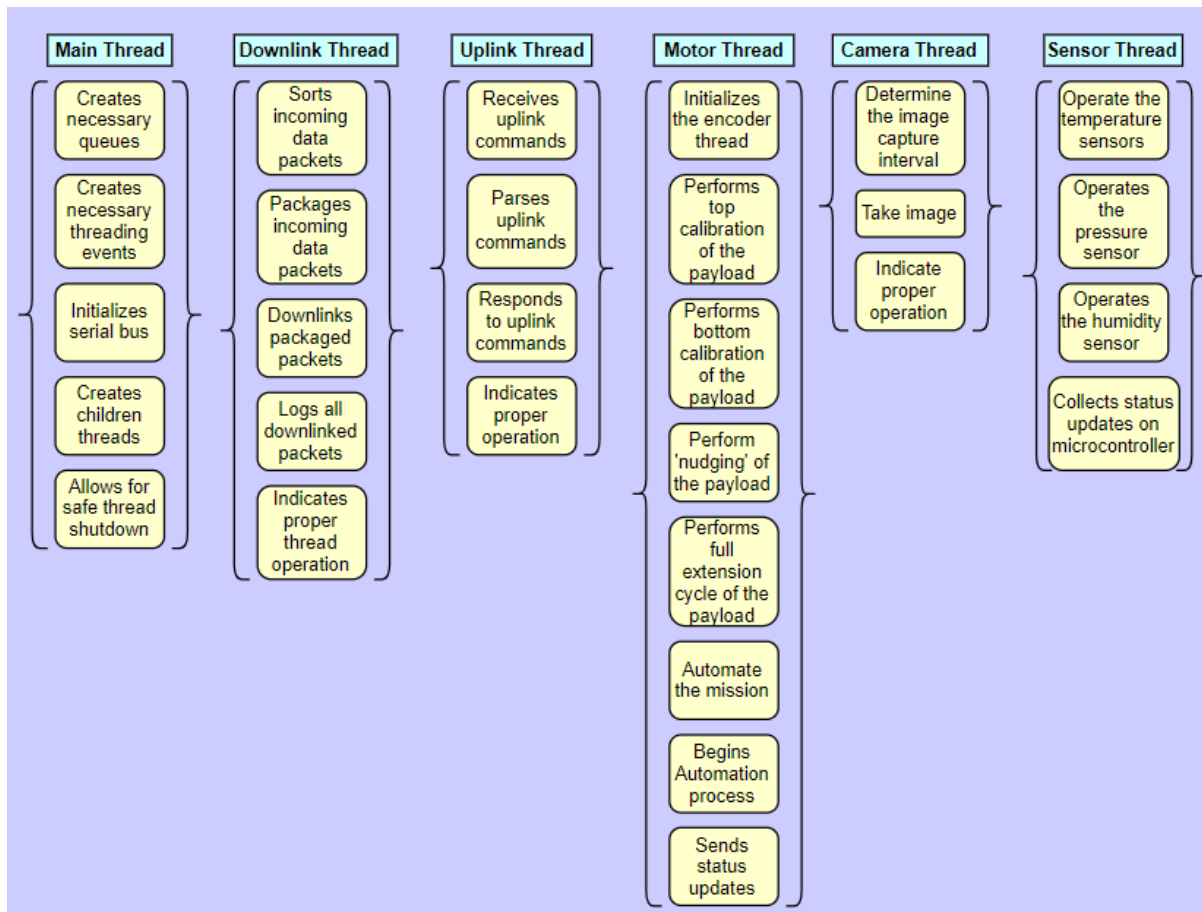


Figure 20: Code Thread Diagram

Main Thread The parent thread: "main" provides the following functionality:

1. Creates queues to allow for communication between threads
2. Creates necessary threading events, which are simple booleans for cross-thread communication
3. Initializes serial bus.

4. Creates children threads.
5. Allows for safe thread shutdown.

Downlink Thread Handles all serial communication from the payload to the ground station, in a process known as downlink. More specifically, it provides the following functionality:

1. Sorts incoming data packets from the downlink queue and logs according to source
2. Packages incoming data packets with predefined headers and footers
3. Downlinks packaged packets over RS-232 bus

Uplink Thread The uplink thread, handles all communication from the ground station to the payload.

1. Receives uplink commands in the form of two-byte messages
2. Parses uplink commands and passes to relevant threads

Motor Thread The motor thread controls all motor movement.

1. Initializes the encoder thread, which monitors the motion of the rotary encoder. This device requires almost constant sampling, hence the separate thread
2. Performs top calibration of the payload refers to the payload extending upwards until a the top button is pressed. It then stores the current step count when the top button is pressed as the “maximum step count”.
3. Move the motor in the prescribed cyclical pattern
4. Perform “nudging” of the payload when the ground team sends a command to move up or down

* An algorithm diagram of the motor thread is provided in the appendix.

Camera Thread The camera thread controls the operation of the camera.

1. Determines the image capture interval based on whether the payload is moving. During motion images are taken in ten second intervals, once per minute while stationary
2. Take an image, cycling through each of the four USB cameras

* An algorithm diagram of the camera thread is provided in the appendix.

Sensor Thread The sensor thread is responsible for all operation of the environmental sensors on the payload

1. Operates the temperature sensors.
2. Operates the pressure sensors.
3. Operates the humidity sensor.
4. Collects status updates on the Raspberry Pi, including core temperature, SD card usage, and CPU usage

2.4.3 Uplink Commands

A set of 18 uplink commands allow for manual operation of the payload for the entirety of the science mission (Table 1). A total of 25 uplink commands were sent during flight for the purpose of troubleshooting.

Table 1: Uplink Commands

Name	Two Byte Command	Description
Ping Pi	0xAA 0x01	Pings payload to test communication
Calibrate Motor Count at Bottom	0xBA 0x01	Retracts payload, resets step count and encoder to minimum value
Calibrate Motor Count at Top	0xBA 0x02	Extends payload, resets step count encoder to maximum value
Min. Success Cycle	0xBA 0x03	Complete 1 minimum success cycle
Full Extension Cycle	0xBA 0x04	Complete 1 full extension cycle
Start Automation*****	0xBA 0x05	Set automation flag as TRUE
Query Safe Mode	0xBA 0x06	Returns ON if safemode is set. Else return OFF.
Reset Step Count	0xBA 0x09	Resets step count to 0
Reset Max Step Count	0xBA 0x0A	Resets max step count to 1500
Query is_open	0xBA 0x0B	Returns ON if is_open is set. Else return OFF.
Turn off is_open	0xBA 0x0C	sets is_open flag to false
Turn on is_open	0xBA 0x0D	set is_open flag to true
Manual Extension and Retraction	0xCA 0x00-0x64	Manual extends to any height, second byte is percent extended
Nudge UpNudge Down	0xDA 0x00 - 0x64 0xEA 0x00 - 0x64	Nudge up or down by specified percentage
Change cycle count	0xFA 0x00-0x03	Adjust cycle type
Safe Mode OFF	0xBB 0x00	Does nothing if safe mode not previously activated. If safe mode previously activated, essentially resets payload to initial state.
Safe Mode ON	0xBB 0x01	Halts motor and sets all relevant flags to false
Reboot Pi	0xDB 0x01	Reboots Pi

2.4.4 Downlink Packets

During flight, data packets from each of the threads were downlinked at a regular rate. The data packets were formatted as follows:

```
CU MI MO SC 1500956918.39 5 50528521 3978
```

- The first term ‘CU’ is a name stamp that HASP uses to give the team the right data
- The second term ‘MI’ is also a name stamp short for Miura used by HASP
- The third term ‘MO’ stands for motor thread but is the place for the name of the thread where the data is coming from
- The fourth term ‘1500956918.39’ is the POSIX time stamp
- The fifth term ‘5’ is the number of bytes of the data being sent
- The sixth term ‘50528521’ is the adler32 check sum
- The seventh term ‘3978’ is the actual data being sent

2.5 Electrical and Power Systems

Electrical and Power Systems supplies the power to the payload, while keeping the devices within operational temperature ranges. HASP provides 2.5 A at 30 VDC during flight.

2.5.1 HASP Integration

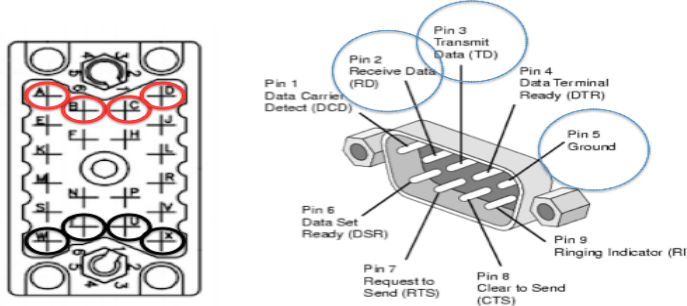


Figure 21: EDAC (left) and DB9 (right)

An EDAC connector (Fig. 21) supplies the power and grounding for the experiment. Pins A, B, C, and D are used for power, and W, T, U, and X are used for ground. The DB9 transmits the serial data to send information back to the ground station.

2.5.2 Power Budget

A power budget was made in order to keep track of the voltage, current, and power, so that the team shall not surpass the supplied amount of power (Table 2). During flight, the current spiked when the cameras turn on and when the motor is moving. The minimum and maximum current are 0.11A and 0.36A respectively, while nominally the current ranged 0.182 ± 0.023 A. HASP power requirements were not violated during flight.

Table 2: Power Budget

Component	Voltage (V)	Current (A)	Power (W)	Uncertainty (W)
USB Cameras (x4)	5.0	0.18	0.90	± 0.10
Environmental Sensors	3.6	0.06	0.22	± 0.04
Raspberry Pi	5.0	0.10	0.50	± 1.10
Stepper Motor Driver	2.8	0.10	0.28	± 0.30
Encoder	3.6	0.06	0.22	± 0.50
Buttons (x2)	3.3	0.03	0.10	± 0.20
LEDs-Strips (x24)	3.3	0.48	1.58	± 0.10
LEDs-Pod (x4)	5.0	0.12	0.60	± 0.10
Total		1.13	4.4	± 2.44

2.5.3 PCB Design

The PCB was designed to have the maximum amount of components with the most efficient use of space. The purpose of the PCB was to organize the way that every component received the correct amount of power from the buck converter. Every device from the power budget above (Table 2) is included on the board other than the motor driver and buck converter, due to the concerns of electromagnetic interference. The Raspberry Pi was directly connected to the board, so the commands can be sent to each sensor efficiently and effectively. Figure 22 demonstrates the Altium design of the circuit board and the populated circuit board (Fig. 23).

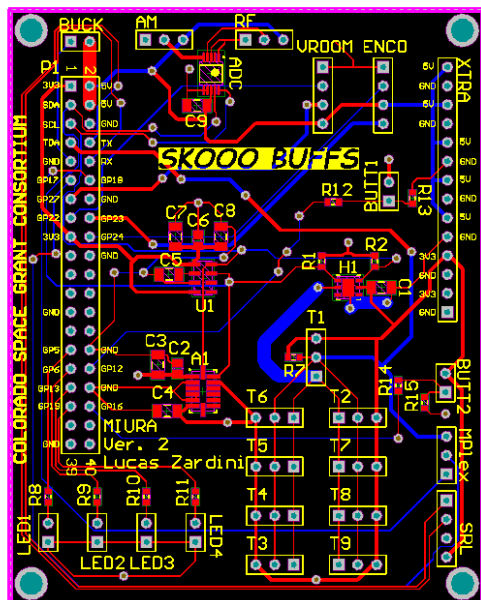


Figure 22: 2D PCB Design

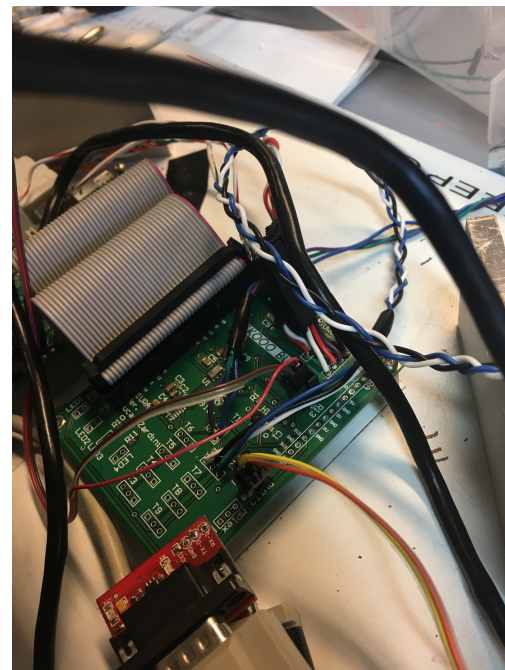


Figure 23: Populated PCB

2.5.4 Wire Management

The largest failure points with wire management were connecting the temperature sensors without interrupting any other connections, due to high number of them (9 sensors). Each sensor was color coded by the wires that determined its placement. For example, figure 25 includes the four indicator LED's along with the camera temperature sensor. The final outcome from the wire management is displayed below in figure ??.



Figure 24: Electronics Housing Wire Management



Figure 25: Wall Wire Organization

3 Testing

3.1 Payload Testing

3.1.1 Tensile Testing

Tensile testing was conducted according to ASTM D76/D76M and ASTM D3822/D3822M guidelines. The purpose was to test the effects of epoxy and small tear formations on the strength of the Kevlar. Kevlar was cut into 1" × 5" test strips and four testing groups were created; plain Kevlar, plain Kevlar with prior tear formation, Kevlar with epoxy, and Kevlar with epoxy and prior tear formation. All samples were folded in the same manner as material at the vertices of the payload. The vertices of the payload experience the highest level of stress and the most wear, and are thus most likely to fail during flight. Epoxied samples were coated with very thin layer of 3M A/B Epoxy similar to what is applied to the final payload. For samples testing the effects of prior tear formation on the payload, small tears were created using an Exacto knife. Prepared samples were placed under tensile forces using an Instron machine until failure.

Kevlar was determined to have a tensile strength that far exceeded the requirements of our mission. It was shown that Epoxy caused a 25% reduction in the strength of the Kevlar, and significantly increased its brittleness. It was also shown that epoxied folded Kevlar broke with repetitive folding (>200 times), and resulted in an 80% reduction in strength from plain Kevlar. Tears in the plain Kevlar did not significantly decrease the strength of the material, nor did they spread to surrounding strands. In the epoxied Kevlar, tears in the Kevlar did significantly decrease the strength of the material (80% reduction in strength), and would spread to surrounding strands.

These results informed design decisions. Since adding epoxy to the Kevlar caused a decrease in strength and flexibility, it was avoided on all creases, except where absolutely necessary to preserve strand placement. Even with this decrease in strength, the epoxied Kevlar was still determined to be of sufficient strength for the parameters of this mission.

3.1.2 Outgassing Testing

Outgassing testing was completed to ensure that any out-gassed material from the payload would not condense on optics and affect camera performance. Additionally there was concern that 3-D printed material may contain air pockets formed during fabrication that could rapidly decompress in low pressures. Testing was conducted by placing a payload model, 3-D printed parts, and a running flight camera in a ball jar with the pressure reduced to 200 Pa, slightly lower than the expected 500 Pa pressure at float. The tested material was massed before and after exposure to the vacuum to test for major mass loss due to outgassing. Camera images were taken throughout the test to ensure that image quality was not reduced. It was shown that there was no visible condensation on optics, and no loss in image quality or clarity throughout the duration of the test. None of the test subjects experienced significant mass loss, indicating no significant outgassing, and there was no rapid decompression of the 3-D material. It was concluded that outgassing was not a concern for this mission.

3.1.3 Optical Testing

The purpose of optical testing was to ensure that flight cameras could capture high-resolution images of the payload in all lighting conditions. Testing was conducted by placing the fully assembled payload in a myriad of lighting conditions. Flight cameras took pictures to be analyzed, and ensure that the needed information could be attained from captured images. Light source attitudes and brightness were changed in order to test the cameras capabilities in the worst possible lighting conditions. Cameras were shown to be acceptably functional in all lighting conditions, however some images were too far overexposed to be viable for use in image analysis. Sample pictures are shown in Figure 26, highlighting images captured with and without significant washout, in both testing and flight. This test provided a good idea of the image quality to expect from flight, and allowed the formulating of image analysis procedures for post flight analysis.

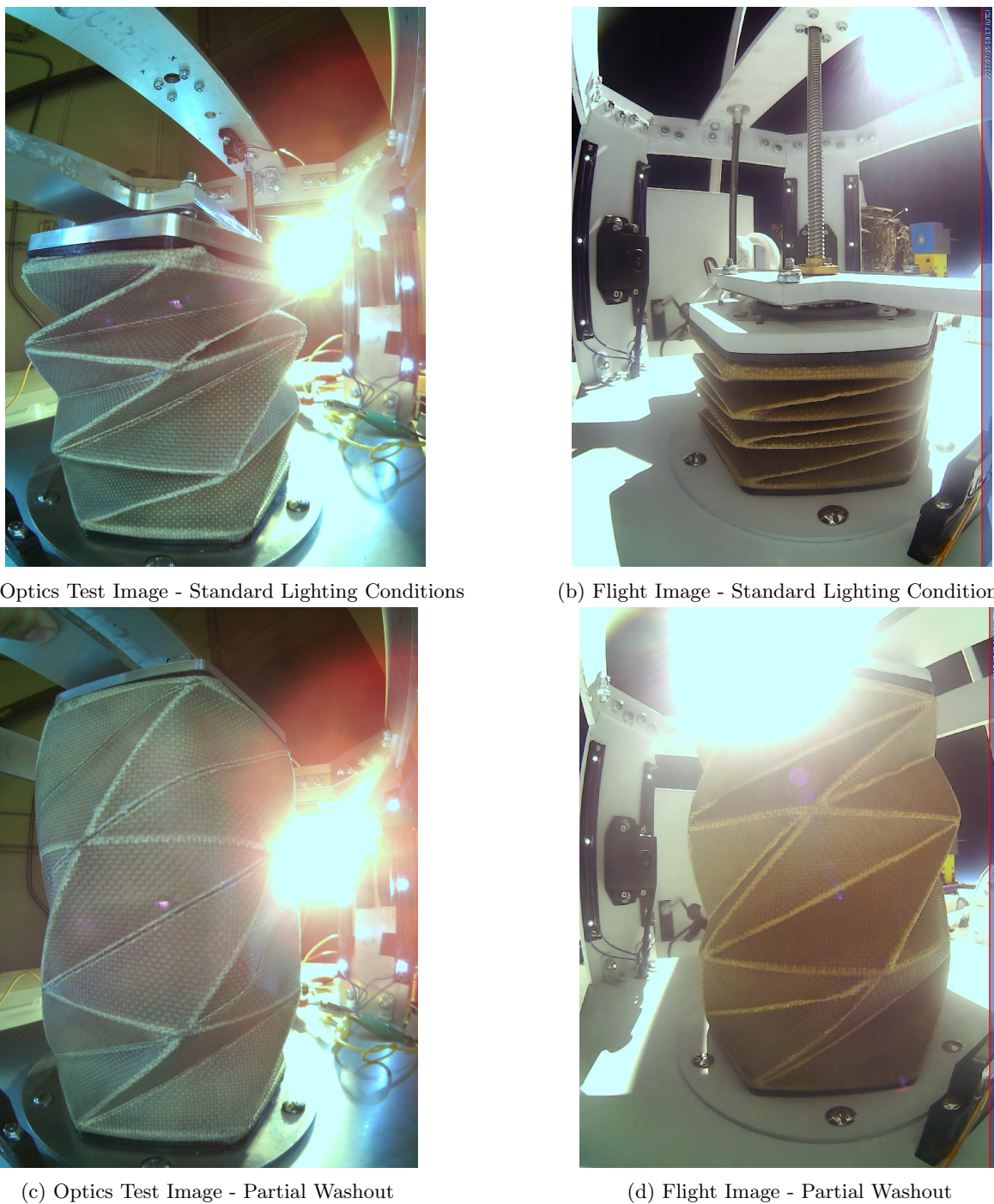


Figure 26: Comparison of Test and Flight Images

3.1.4 Thermal Testing

The purpose of the thermal testing was the verification of the payload's performance in temperature extremes that it would experience in flight. During ascent the payload passes through layers of the atmosphere with temperatures as low as -40°C , so it was essential that the payload be able to successfully operate in these low temperatures. The payload was placed in a cooler in its compact orientation with dry ice to lower the temperature to -40°C . The payload ran for two hours successfully demonstrating acceptable performance throughout the test. It was noted, however, that the upper button should be lowered 0.5 cm to ensure that the payload would consistently press the button in cold temperature conditions. Additionally it was shown that there was an increase in rigidity of the Kevlar due to the extreme temperature conditions. These effects were tested and analyzed more in-depth during

post flight analysis.

3.2 Systems Testing

The purpose of the Day in The Life testing was to verify nominal operations of all systems of the payload for a duration, and in lighting scenarios similar to those on flight.

The test was conducted by placing the fully assembled payload outside in the Sun and powering it on as it would be in flight. As per flight code, two hours into the test the payload began cycles and pictures and data were recorded. Minimum success criteria and data were recorded and met early in the test. Cycles continued into the night in order to test the night time environment expected at flight. The test concluded after 12 hours of nominal system performance.

3.3 Integration Testing

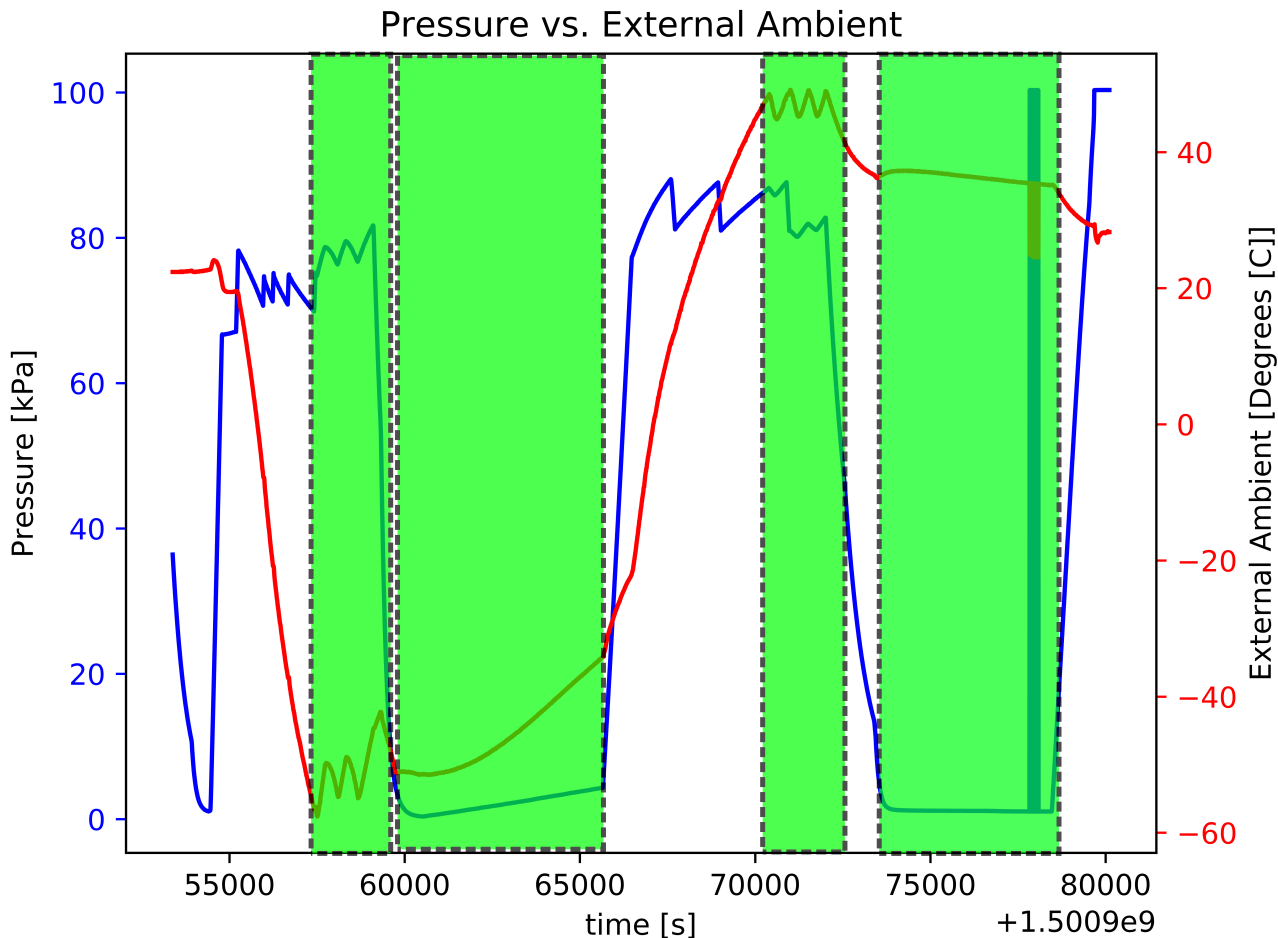


Figure 27: Conditions during TVAC. Blocked regions show, in left-to-right order, high pressure and low temperature, low pressure and low temperature, high pressure and high temperature, low pressure and high temperature.

Integration testing with the HASP platform occurred at the Columbia Scientific Balloon Facility in Palestine, TX. Each of two tests in a TVAC chamber followed the temperature and pressure profiles shown in Figure 27.

During the first TVAC test, the payload operated as expected, but failed to reach the upper limiting button during the cold sections of the test. After further testing during before the second TVAC test, the team modified the flight code to overestimate the maximum required number of steps for extension. During the second TVAC test, no further issues were encountered and the payload operated as expected.

4 Flight Overview

4.1 Timeline

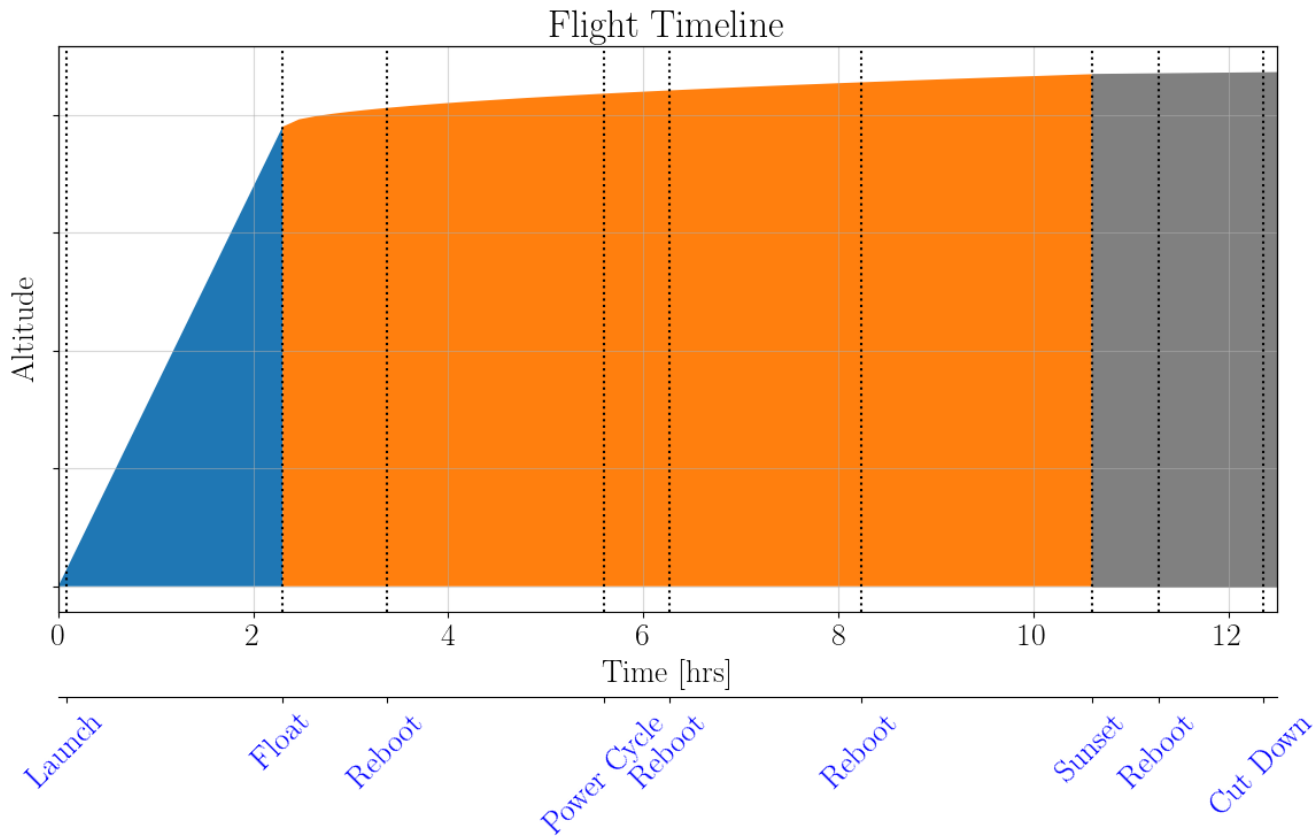


Figure 28: Major flight events with platform float pattern, showing ascent (blue), day-time float (orange), and night-time float (gray)

Launch operations began around 3 a.m. on September 4th, 2017. The mission did not begin until float altitude, when the flight team sent a command to begin extension cycles. The calibration cycle and the first full extension cycle were completed without issue, but the payload was unable to extend again. For the remainder of flight, the launch team attempted to troubleshoot what may have occurred, and sent variations of commands in hopes that the data would be useful for post-processing.

Table 3 duplicates the notes from the flight team's notebook, with Figure 28 showing the major milestones overlaid over rough flight altitude.

Table 3: Launch timeline, drawn from flight team notebook

8:30 MDT Launch, flight time T+00:00

10:33 MDT Float altitude reached

10:34 MDT Sent command to begin extension cycles

10:36 MDT Calibration cycle

11:20 MDT First cycle completed, successful extension, retention, and retraction

12:01 MDT Noticed discrepancy in encoder data; payload did not extend for scheduled second cycle

12:20 MDT Flight team discussed options, decided to send reboot flight computer command

12:33 MDT Sent command to extend payload to maximum extension, no movement

12:40 MDT No movement visible on CosmoCam

12:45 MDT Tried other nudge commands both up and down, still no motion on CosmoCam

12:50 MDT Checking current from HASP data, comparing environmental conditions before and after failure

13:41 MDT Compared encoder plots to TVAC data, reviewed notes from pre-flight to ensure all procedures were followed

13:43 MDT Command sent to recalibrate payload at top button, current spiked to 270 mA from nominal 200 mA

13:55 MDT Power cycled entire payload using HASP command

14:04 MDT Sent commands to reset cycle count and restart automation

14:11 MDT Rebooted flight computer again

14:22 MDT Mission start command sent

14:28 MDT Still no payload movement, confirmed command was received

14:31 MDT Leading theory is that guide bar shifted and became stuck

14:44 MDT Cycle command sent again

14:48 MDT Safe-mode command sent to halt cycle code execution, planning on attempting to “wiggle” guide bar loose

15:00 MDT Rebooted flight computer

15:06 MDT Sent several up/down motor nudge commands to attempt to unstick the guide bar

16:12 MDT Unsticking payload with various nudge commands unsuccessful

16:15 MDT Hooked up backup motor attempting to reproduce the problem on the ground. Concurrently other members of flight team sent various commands to observe the effect on current draw

19:01 MDT Collected data on current draw when motor moving, no discernible pattern. Unable to reproduce problem on backup motor. Now sending various combinations of commands (nudge up five times, nudge down five times, etc.) in hopes that some pattern will appear in post-processing

20:45 MDT Announced cut-down, mission end

5 Results and Analysis

The two main focuses of analysis were to determine the root cause of failure, and use the data collected during testing and flight to characterize payload performance within the environmental conditions of flight. To characterize the performance of the material, the design was analyzed for compactability and reliability of folding through multiple extensions. The material was analyzed for durability by examining hole and tear formation, and how well it supported the design implementation. Overall both the design and material performed remarkably well. Improvements could be made however, and these are detailed in subsequent sections.

5.1 Environmental Results

The environmental sensors from which data was taken during flight comprised of temperature (External: Fig. 29, Internal: Fig. 30), pressure (Fig. 31), and humidity (Fig. 32). The calibration cycle and subsequent extension cycle occurred during the 30 minutes after reaching float, designated by “Float” on the plots below. External and Internal temperatures increased during this time, but pressure and humidity remained constant during both cycles.

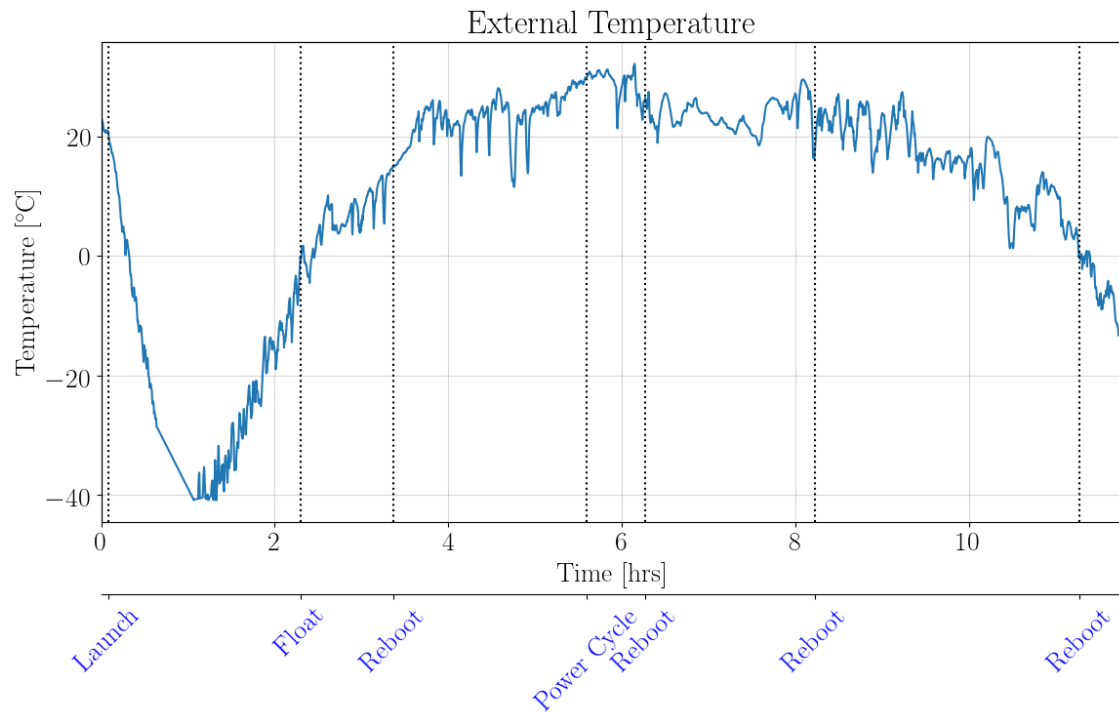


Figure 29: External ambient temperature through duration of flight

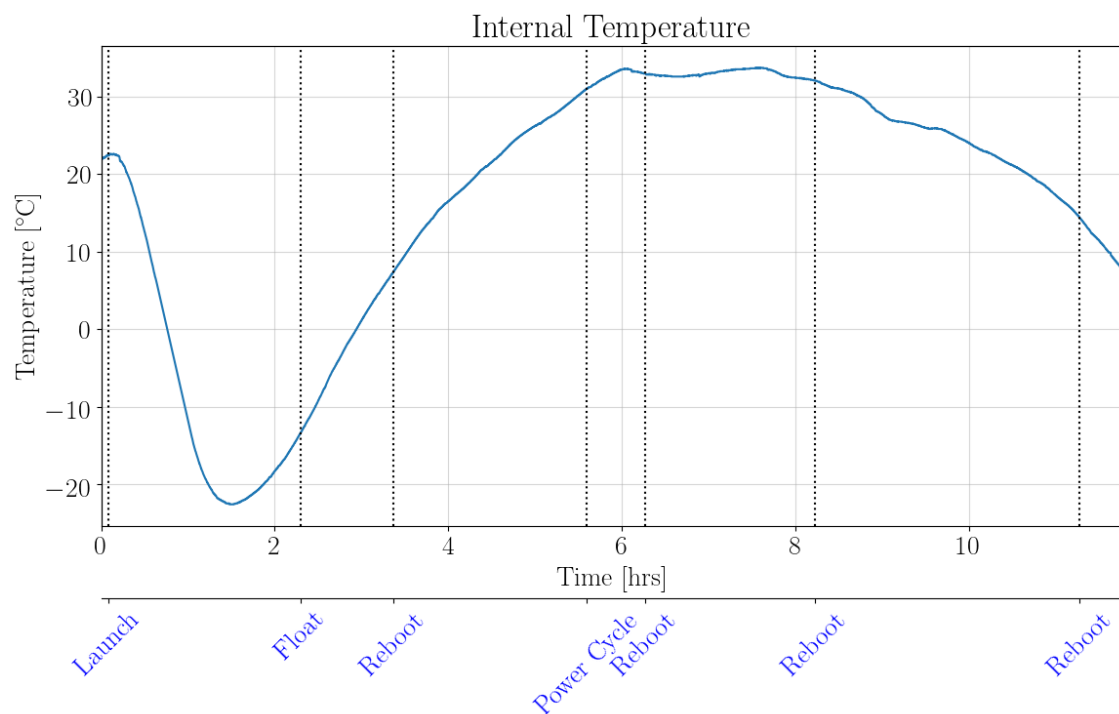


Figure 30: Ambient temperature of the electronics housing through duration of flight

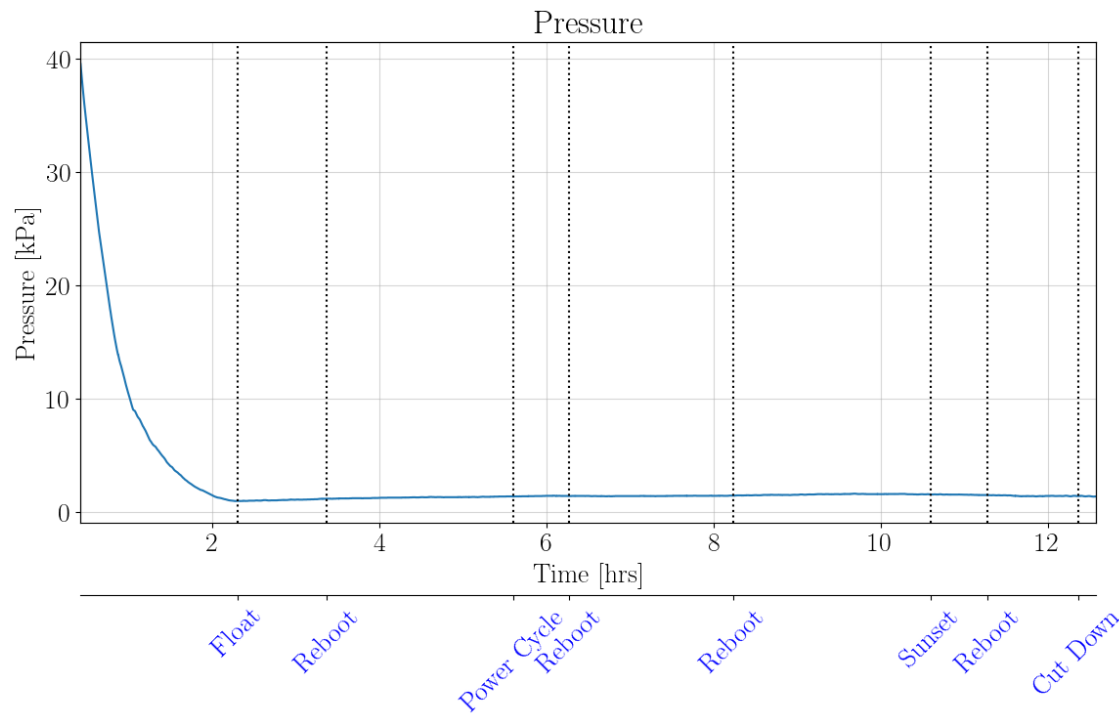


Figure 31: Pressure through duration of flight

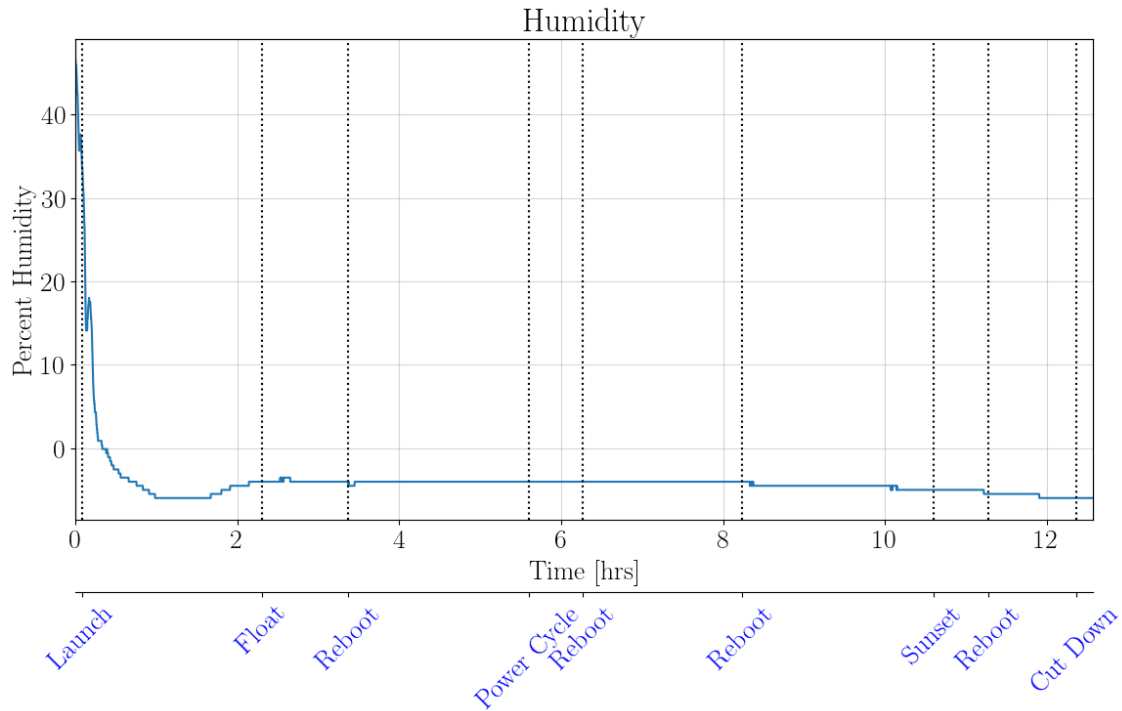


Figure 32: Humidity through duration of flight

5.2 Root Cause Analysis

5.2.1 Initial Possible Causes

Figure 33 is a visualization of the possible causes for failure during mission. Once each possible cause for failure was identified each cause was looked into more in depth and determined to be credible or not. Similarly, initially the team looked into environmental data to determine whether or not the failure was because of those conditions. Figures 34, 35, and 36 compare position of the extendable structures to different environmental conditions. It was determined that the conditions did not change a concerning amount of time between when the payload was functioning and when it failed. Therefore, environmental conditions were ruled out at the beginning.

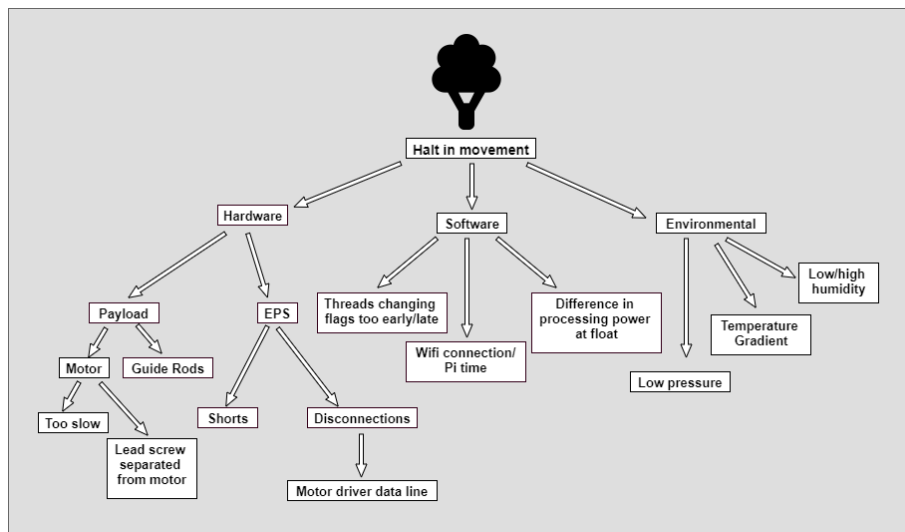


Figure 33: Root Cause Analysis

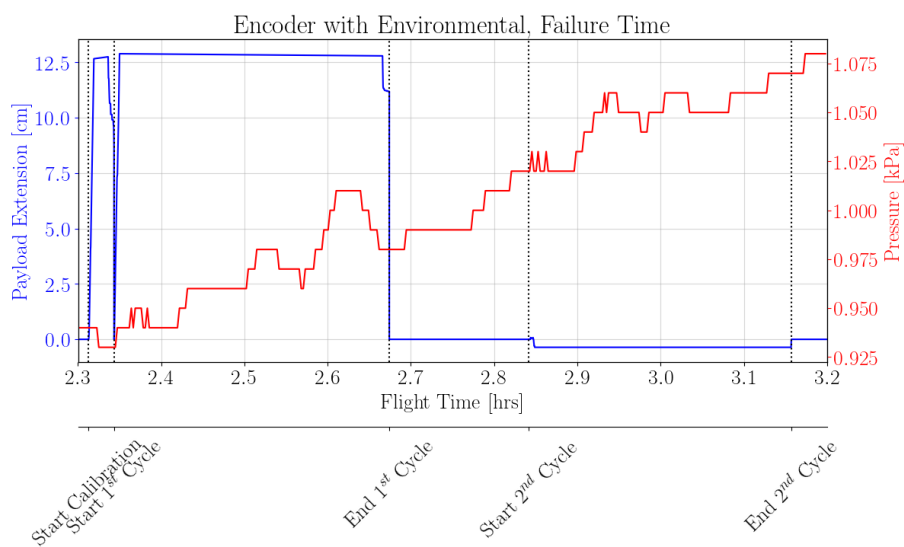


Figure 34: Extension with Pressure Overlayed

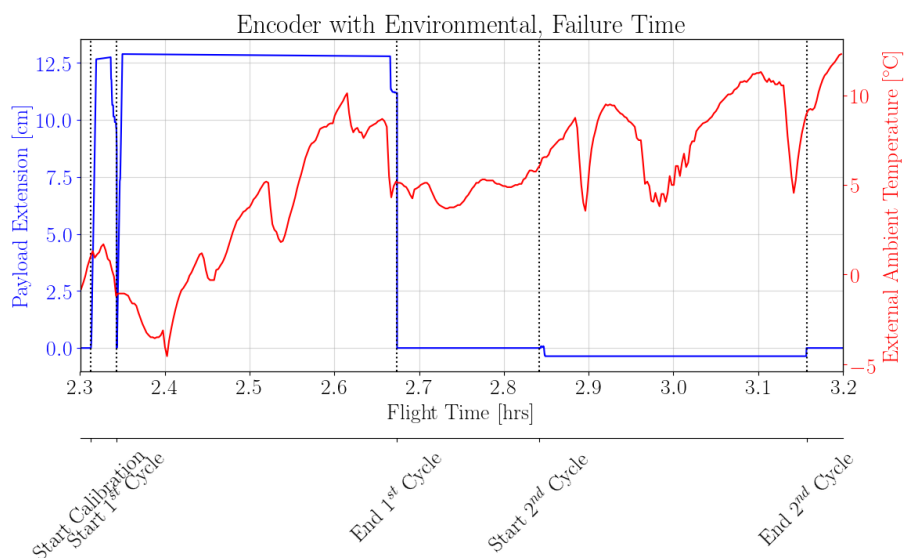


Figure 35: Extension with Temperature Overlayed

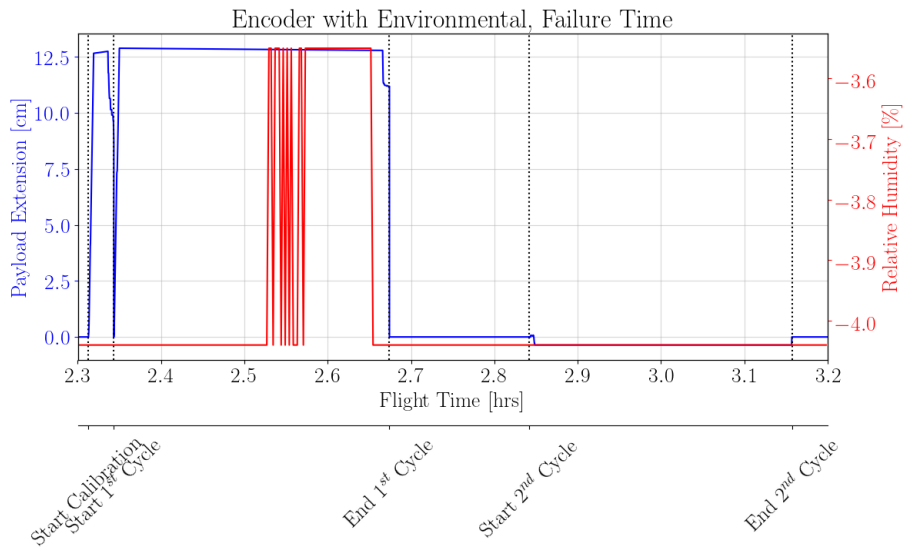


Figure 36: Extension with Humidity Overlayed

5.2.2 Motor Driver Test

The motor driver was suspected as a failure point for the mission, so a prototype was made for testing. The test consisted of unplugging the direction and step pins in various combinations to observe the characteristics and current of the motor. Table 4 below demonstrates the results from a single motor and motor driver being powered with 6 VDC and 0.19 Amps. The results show that the motor driver has two states when either pin was unplugged, no movement or only downwards movement. The current only changes when there is no movement, due to the lack of communication of the motor driver to the motor.

Table 4: Motor Driver Data

Pins Pulled	Current (A)	Movement
Step in/Dir in	1.19	Yes (downwards only)
Step out/Dir in	1.12	No
Step in/Dir out	1.19	Yes (downwards only)
Step out/Dir out	1.13	No

5.2.3 Failure Analysis

From the motor driver test, the final hypothesis of the mission failure is caused from the motor driver. When the direction pin is not attached, the motor will only go one direction, downwards, because that pin is pulled to ground. Due to the lack of direction in the motor, the commands that the CDH team sends will not affect where the payload will go. This means that the motor will go down until it reaches the button and stops, until it becomes fully pressed. Once the next cycle starts, the motor will get stuck as it will try to keep going down, although it is on the button. This will cause the current to stay the same, while the payload stays in the folded position during the rest of flight.

The reason this could happen 2.7 hours into flight is if there is a cold solder joint or bad connection with the Molex connector. This would be the case, because it could work for some time, but then lose connection due to the thermal conditions in the stratosphere.

After recreating the situation from flight, by disconnecting the direction pin, the payload reacted identically to what was seen on flight. The current did not change, while the motor descended to the button, and then got stuck for the remainder of the test. Further analysis shows that the Molex connector was not stable due to the lack of precision in soldering the direction pin on the PCB. This was proven by observing the connectors and solder joints and noticing the lack of connection in some states when probing the direction pin solder joint with a multimeter. This signifies a bad solder joint, waiting to break the circuit at any given moment. The reason this was not noticed

before flight was because there were no vibe, drop, or any tests that could cause that direction wire to come apart from the PCB. The solder joint of the direction pin can be seen in Figure 37. This picture is from post flight, and the direction pin is the purple wire (second pin down from the top). The joint does not seem to be secure by solder and looks fragile, therefore causing failure during flight.

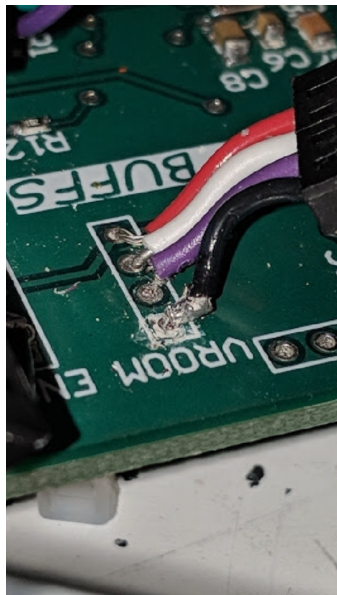


Figure 37: Bad Soldering Joint

5.3 Extension Cycles

The flight model underwent an estimated 300 cycles over the course of testing and flight. Approximately 70 cycles were completed during TVAC testing, 20 cycles were completed in a cold environment (-60 – -30 °C), and 13 cycles were completed in a hot environment (30-60 °C). The final 2 cycles were completed during flight in the near-space environment.

5.4 Material Analysis

Material analysis was completed with the purpose of characterizing performance of the Kevlar-Epoxy material in a near space environment, and to determine how well it adopted the origami folding design. The main purpose of Miura was to determine the viability of a reusable structure. As defined in the system requirements and success criteria, a material failure would be observed when a hole larger than one square millimeter formed on the payload material during flight. The following sections will outline the procedure used to document any material damage and the material's viability for future missions. A controlled tear was created on a non-critical corner of the payload to serve as a reference for what a material failure would look like post flight.

5.4.1 Post-Flight Visual Inspection

The payload was received by Colorado Space Grant on the 15th of September, 2017. After being carefully unpacked and checked for massive damage, the Kevlar-epoxy material was inspected for any large rips or tears. As noted earlier, a test tear was created that would serve as the reference point for material failure. Figures 38 and 39 below show the reference tear both during and after flight, also comparing it to a non-damaged corner.

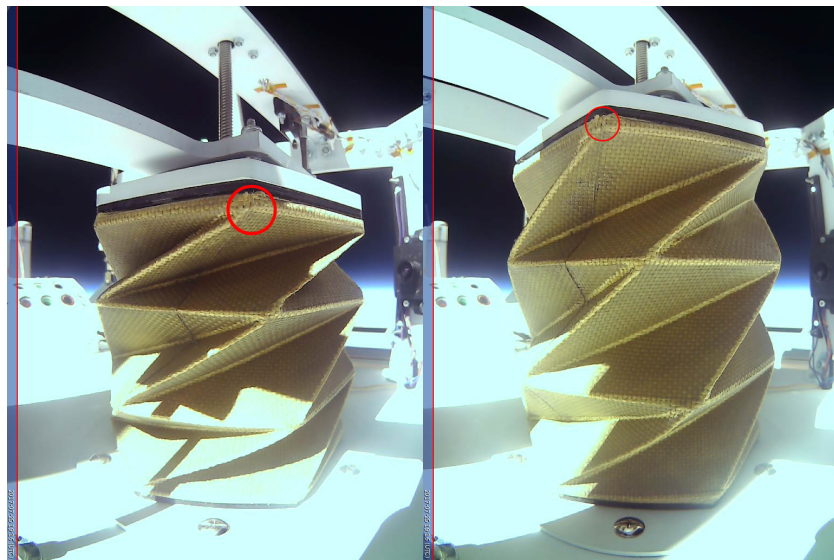


Figure 38: Images taken by cameras during flight showing reference tear.



Figure 39: Images taken post flight showing reference tear in red. A normal, non-damaged corner is shown highlighted in green for comparison.

Under visual inspection, without the aid of magnifying lenses, the material had no visible failures. As a one square millimeter hole or tear would be noticeable by the human eye, this means that the payload material itself successfully completed the mission and is viable for a reusable, folding, extendable structure.

5.4.2 Post-Flight Magnified Inspection

Although no material failures were visible to the human eye, it is still important to characterize how the payload material would perform over time. It is important to note that the payload material flown on HASP had extended and contracted an estimated 300 times prior to flight. These extensions took place throughout subsystem testing, and most importantly TVAC testing.

To further inspect the materials for any damage such as fiber separation or micro-tears, the use of a stereo microscope was employed. This would allow a much closer look at any holes beginning to form or individual Kevlar fibers tearing. The figure below illustrates how a failure-inducing tear would look under 30x magnification. Figure 40 shows a reference tear placed on the payload before flight at 30x magnification.

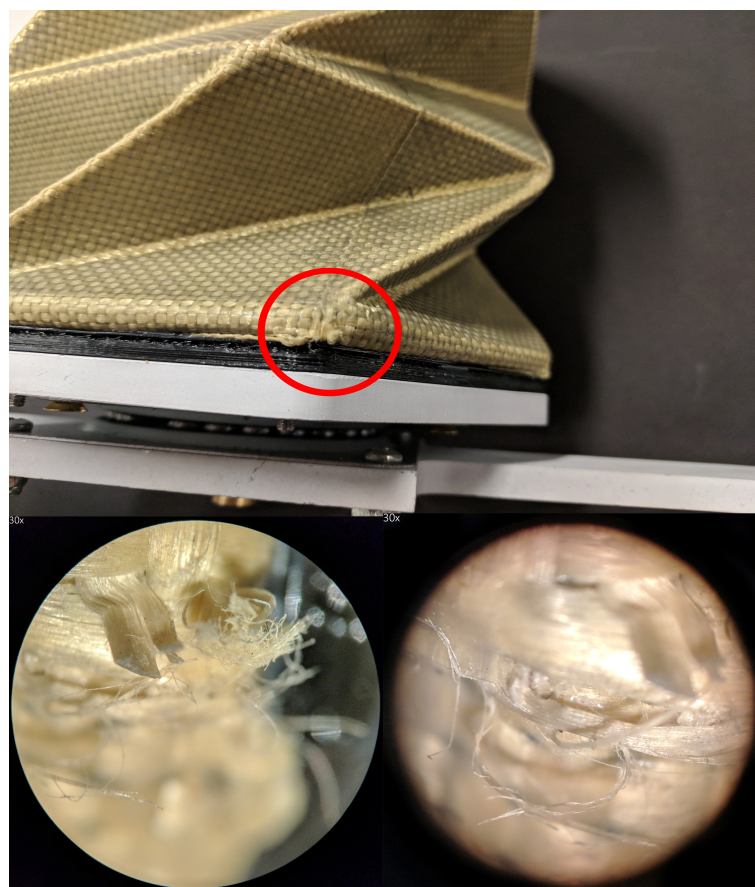


Figure 40: Images taken post flight showing reference tear in red. Images taken at 30x magnification show that any tear would be noticeable under magnified inspection.

It is quite clear that if the material did fail, it would be abundantly obvious when the microscope was used. The surface of the payload was divided into four main surface types. The first are the flat, triangular, epoxy reinforced planar surfaces (Fig. ??).

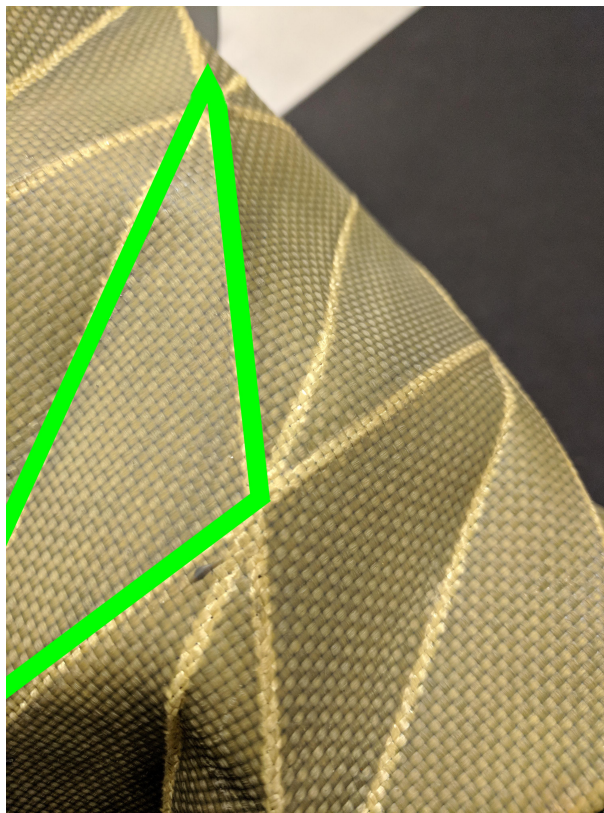


Figure 41: Images taken post flight highlighting in green a single epoxy-reinforced face.
??

These reinforced faces are the least likely to fail, as they stay relatively fixed throughout extension and retraction. During the last 74- 100% of extension, they transition from completely flat regions to curved slightly outward, but experience very little stress or strain in the process. Visual inspection with the naked eye yielded no holes or tears being found. Use of the microscope supported this claim, finding that all flat faces remained in pristine condition. This means that no Kevlar strands separated, no holes formed, and no individual Kevlar fibers tore. Figure 42 below shows one flat face under the microscope.

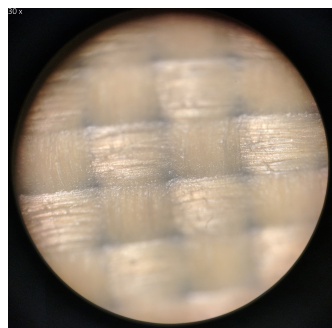


Figure 42: Intact weave on planar region

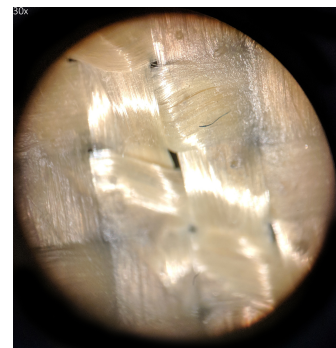


Figure 43: Shifted fibers on crease showing potential for hole formation

Figure 42 above makes it clear that all strands and fibers remained intact on planar regions, holding the same form throughout testing and flight. The thin, translucent gray layer of epoxy can be seen on top. These faces were expected to behave this way, as they experience only minor deformation during flight.

The next surface type is the interior folding boundaries ('valley folds'). These are the strands of Kevlar that are not held in place by epoxy and fold inwards when the payload is in its retracted state. As these lines are not

reinforced, slight rearrangement of Kevlar strands was expected. That was not the case. These interiorly folding ridges performed remarkably well, with no holes visible at 30x magnification.

The next surface classification is the non-reinforced Kevlar creases that fold outward during contraction ('mountain folds'). Because of the folding design, these creases are forced to compact twice as much as the interior folding creases in a compacted form. As a result, These ridges experienced a much higher strain. Because of this, it was expected that these ridges would take some damage over time, resulting in deformation of Kevlar strand arrangement or the possible tearing of a Kevlar fiber. The image below shows a magnified view of one of these outward facing ridges. It can be seen that although there are no tears of the Kevlar fibers themselves, the strands have been deformed. This deformation results in the strands no longer being straight, and in turn beginning to form small holes on the scale of one tenth of a millimeter in diameter. Because holes were defined as a shift in fibers at least one millimeter in diameter, these micro-holes are not considered a material failure. Their presence does reveal how the material is stressed, however, and reveals the potential for hole formation.

The final surface classification is the vertices or corners of the payload where the creases meet. These regions experience the highest stress of any region, as the fibers are forced to fold completely in half and are pulled in opposing directions. If the fibers are left unsecured, large holes would begin to form directly on either side of the vertex, as shown in figure To mitigate hole formation, fibers are held in place by an extra layer of epoxy, and thus experienced no shifting during flight.

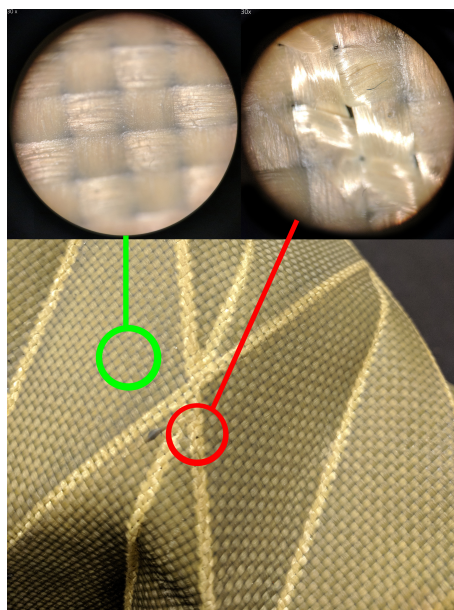


Figure 44: Images taken post flight at 30x magnification showing an unreinforced, outward folding boundary. Note the small hole due to misalignment of fibers.

These outward folding ridges performed better than expected, experiencing only minor strand deformation and no fiber tearing. As said earlier, this payload has undergone almost 300 extension and retraction cycles. This same payload has been used in all of those cycles, meaning that only the tiny hole pictured above formed only after extended repetition and stress. The payload did not experience a single critical failure over a massive amount of cycles allowing us to classify the material as well-suited to the folding design. Additionally the use of just one piece of material eliminated the need for extensive seams and created fewer failure points than other fabrication methods may have been able to achieve.

5.5 Thermal Behavior

During an orbital deployment of a soft-shell module, different sides of the module would experience vastly different temperature extremes. This could potential lead to expansion and contraction of the material on different sides, and unpredictable and uneven deployment. Thus, it is extremely important to begin analyzing the thermal behavior of the selected structural material. The payload experienced a large range of temperature extremes throughout testing and flight. The most prominent effect of different thermal environments on the model is the change in flexibility of

the material. It was observed in the first cold test that the payload noticeably stiffened in an environment colder than 0 °C. This stiffening effect increased the amount of force required to both fold and unfold, and was most noticeable in the region of deformation, from 70-100% extension.

This stiffening effect was analyzed and tested post flight. The payload was placed in a cooler with dry ice, and the force required to extend the payload at different points in extension was measured for each temperature. It was found that the force needed to fully extend the payload at -40°C increased to 220 % of the force required at 20°C. During pre-flight testing, it was observed that the epoxy was the part of the material that was stiffening in the cold thermal environment. The stiffened epoxy on the vertices resisting both folding and unfolding, and the epoxy on the planar regions prevented them from fully deforming, or “puffing out” at 100% Extension. The screw drive was unable to supply the required force, and thus the payload was unable to extend or contract as far as theoretically proposed.

To combat this stiffening and resulting slight decrease in performance, thermal insulation of the payload was considered before flight, but ultimately rejected because any thermal insulation or other exterior layer would have obstructed visual analysis of the structural layer. The inability to add thermal insulation to the payload lead to a decision to decrease in the amount of epoxy on the creases for the flight model. Only the minimum amount required to preserve strand placement and increase stability was used.

5.6 Design Analysis

The overall model design was chosen for simplicity since this was the first mission of its type for COSGC. The relatively simple design decreased potential failure points, was reliable, and allowed for more time to be invested in material research and analysis. However the design is an over-simplification and does not perfectly model a spaceflight ready design. These details are expanded upon in the following sections.

5.6.1 Origami Design

The helically triangular cylinder design vastly outperformed expectations in multiple regards. Though many early revisions experienced numerous deformations, the flight model did not deform once in over 300 cycles. The only deformations that occurred were the planned flexing of the planar regions during the last stage of extension. No unplanned deformations occurred during the entire lifetime of the model. The rotational aspect added stability in the x-y plane during extension, and lead to an even extension across all rows.

Some limitations to the design include limitations to packing ratio, and sharp angles result in high stress on material at corners and vertices. The sharp vertices lead to the beginning of hole formation for unepoxied regions. Additionally, if pressurized, pressure would increase greatly at corners and vertices, only adding to the stresses on the material. The cylindrically-based expanded design would also lead to an increased pressure build up at the edges of the bases. The rotational aspect of the design increases stability, but also increases complexity if mechanical assistance is required for expansion or retraction. Lastly, the design does not allow for contraction in the x-y axis directions, only along the z-axis direction. This means that the retracted diameter is identical to the expanded diameter, and any module based upon this design would be limited in width by the fairing dimensions of the launch vehicle. This limitation also limits the packing ratio, discussed below.

5.6.2 Packing Ratio

A soft sided structure is selected for spaceflight based upon its low weight, and packing ratio (low launch volume to high expanded volume ratio). Since only the structural layer was designed and flown, weight was not considered. The packing ratio was analyzed for project Miura, and the results are reported below in Table 5. The theoretical achievable dimensions for the design are displayed in the left column, and the dimensions actually achieved during flight are displayed on the right. It can be seen that the payload was unable to fully extend or retract to the theoretical dimensions. This was due to stiffening of the material during flight, discussed previously in section 5.5.

Table 5: Comparison of Theoretical and Achieved Packing and Extension Dimensions

	Theoretical	Achieved
Extended Length [cm]	18.5	17.6
Retracted Length [cm]	2.40	2.90
Expanded Volume [cm ³]	338	322
Compacted Volume [cm ³]	43.9	53.0
Ratio of Expanded to Compacted Volume	7.70	6.07

For comparison to current deployable structures, the theoretical dimensions have been scaled up to match the length of the Bigelow Beam Module. Its theoretical dimensions and packing ratio are compared below. The first column reports the theoretical dimensions of the Miura model flown, the second column lists the theoretical dimensions and ratio for the scaled model, and the last column reports the dimensions and ratios for the Bigelow Beam Module [1].

Table 6: Comparison of Dimensions of Miura Model, Miura Scaled Model, and Bigelow Beam Module

	Miura	Miura Scaled	Beam Module
Extended Length [m]	0.185	4.00	4.00
Retracted Length [m]	0.024	0.52	2.16
Extended Diameter [m]	0.13	2.81	3.23
Retracted Diameter [m]	0.13	2.81	2.36
Extended Volume [m ³]	0.338	24.8	16
Compacted Volume [m ³]	0.043	3.22	1.4
Ratio of Volumes	7.70	7.70	11.4

From Table 6, it is apparent that the Bigelow Beam Module is far ahead of the Miura module in terms of compressibility. It must also be noted that Miura only flew a single structural layer, as opposed to a multi-layered module. Miura's design was not able to achieve as high a packing ratio for the following reasons: when scaled down, materials do not fold as effectively, Miura's design contracted in the z-axis direction only, and had a large empty section in the center when compacted. This section was necessary to allow the screw drive to pass through, however the space was larger than necessary. With design changes however, Miura origami would still be a viable alternative to other packing methods, and could allow for retractability while maintaining a comparable packing ratio.

5.7 Material Accommodation to Design

An origami-style fold is not Epoxied Kevlar's natural state, thus it is important to analyze the material's ability to accommodate the desired design. The Epoxy-Kevlar composite material has a much lower toughness and flexibility in comparison to plain Kevlar. For this reason, epoxy is not well suited for the creases and vertices from a material properties standpoint, but is necessary to prevent the shifting of fibers and formation of holes. Without epoxy reinforcing the seams, there was also a risk of creases and vertices buckling, instead of folding. Thus some amount of epoxy is necessary on creases, but the amount must be tightly managed and the placement carefully considered to avoid creating weakness on the creases.

An additional area of consideration is the weave density and strand thickness. If the weave density is too low or the strands of Kevlar are too large for scale of the model, the strands are more susceptible to shifting. This can result in hole formation. The weave used for the Miura model had a high weave density, but also a large strand size, and was thus susceptible to fibers shifting. For comparison, if model was scaled to the size of the Bigelow Beam module (4.01 m length, 3.23 m diameter), each thread would be 2-3 cm thick. This is far too large for the scale.

A weave of finer strands was considered, however it would not have provided the necessary rigidity and strength on its own, and would have necessitated multiple layers. For this mission, multiple layers were avoided, however for future missions, when direct visual monitoring of the structural layer is not necessary, multiple structural layers of a high weave density and small strand size are recommended.

6 Conclusions

6.1 Mission Objectives

Mission Objectives

1. Extend, sustain, and retract a durable, foldable soft-shell structure multiple times in a near-space environment.
2. Quantitatively monitor the extension, retention, and retraction of the soft-shell structure.
3. Capture high resolution images to analyze the soft-shell structure's deployment process, retention of the extended state, and retraction into a compact form.

6.2 Minimum Success Criteria

Below are the project's minimum success criteria which define what would qualify as a successful mission. The criteria is met unless it is red. The reason that the second success criteria was not met was due to the fact that the Payload was only able to sustain itself once during flight. This occurred because the payload was programmed to run a "calibration" cycle which was just an extension and contraction with no sustention. When the payload was not able to extend again after a calibration cycle and a normal cycle it meant there had been two extensions, two contractions, but only one sustention.

Minimum Success Criteria

1. Extend the soft-shell structure to at least 70% of its maximum height without tearing, twice during flight.
2. Sustain the soft-shell structure at 70% or higher of its maximum height without tearing, twice during flight.
3. Contract the soft-shell structure from 70% or higher to 10% or lower of its maximum height without tearing, at least once during the flight.
4. Capture one discernible high resolution image from each of the four angles at apex of the second or a subsequent extension stage.
5. Record positional data at the beginning and end of both extension stages.
6. Record positional data at the beginning and end of the contraction stage.

6.3 Requirements

Below is a list of requirements that were not met. The full list is in Appendix D. Apart from the first requirement in the list below, which failed because of the halting of cycles, the other five requirements were not meant due to a de-scope in mission during building. Towards the end of the project as the deadline to ship approached, there were many things to complete and some of the tasks were not mission critical. By cutting out those tasks, such as downlinking images, the team was able to focus on completing the more mission critical tasks.

Requirements That Were Not Met

- 0.1 The payload shall extend, sustain, and retract a foldable soft-shell structure multiple times.
- 0.4.3 The payload shall measure and record the acceleration of the entire payload at least once per second.
- 0.4.5 The payload shall measure the motor's current draw at least once per second.
- 0.5.4.1.1.1.1 The payload shall downlink visual data to the ground.
- 0.5.4.1.2.1.6 The payload shall be capable of receiving and executing a command to downlink an image.
- 0.5.4.1.3.3 The payload shall downlink an acknowledgement for each command that fails execution.

6.4 Overall System Functionality

While Miura did not meet 1 of the minimum success criteria and 7 of the requirements, the mission was by no means a failure. The issue that caused the halt in extension cycles was determined to be electrical and therefore not caused by the design of the extendable structure. With the constant functionality of every other vital system on the payload for the entire flight, much data was collected while the structure was extending, sustaining, and contracting. This visual and numerical data was more than sufficient to decide that the Kevlar-epoxy composite was extremely durable enough as a structural for space missions and will not tear or form holes easily. Likewise, the folding design was determined to reliably return back to its original form and not have any folds invert on at least two occasions. This data and lessons learned will be pertinent for future extendable structure missions from the University of Colorado and from any other institution.

7 Lessons Learned and Recommendations

7.1 Payload

After the fabrication process and flight testing of the payload there were many important lessons learned. Initial materials research for the payload was misguided, and some important material properties were not considered, most importantly with considering the future application of the payload as a space habitat. Materials researched had the correct properties for use in the origami design, but would not have served well as for a living module. This delayed the payload's design process and led to future errors. If the project were to be re-done it would be important to consider the future of the project beyond just immediate mission success criteria.

More consideration and planning needed to be put into the fabrication process, as for this mission it was largely trial and error based past a certain point. This process should start earlier in the design phase, so that by the build phase, the fabrication method has already been developed.

Each layer and design iteration should be tested more fully pre-flight in different environmental conditions, and its behavior understood before launch. This will limit the need for chunky monitoring systems during flight, and will limit the need for individual monitoring of each layer, which would not be feasible for a mission with multiple layers. Along these lines, sensor type and placement should also be carefully considered to ensure sufficient monitoring of the structure, and that useful data is being gathered that will be of benefit during post-flight analysis.

7.2 Structures

The most important lessons learned in regard to engineering the structural components of this mission stem from team collaboration and translation from CAD models to a physical component. The most commonly used CAD software available to students at the University of Colorado is Solidworks, developed by Dassault Systemes. Operating under a student license, it is nearly impossible to set up Solidworks Product Data Management, the feature used to allow real-time collaboration on CAD models. Early in the semester, collaboration was done by creating numerous copies of component models and having a team member work on them individually. This led to confusion, miscommunication, and stress that all could have been avoided by switching to a cloud-based CAD system. The structures team switched to the online software OnShape, allowing all team members to work on components and designs at one time. This improved collaboration expedited the overall design process, allowing important resources to be used elsewhere.

It is incredibly easy to implement structural components such as bolts, screws, and brackets from software toolboxes into a CAD model, but this software ease does not translate into real life ease. Re-ordering and redesigning components can be time consuming and costly, so it is important that the real-life application of any part is thoroughly considered before adding it to a computerized model. Finally, a structure should be designed so that it is easy to both assemble and disassemble. Many payload components were very easy to install the first time around, but as components were added, connections and different areas became difficult to reach. In an ideal situation, no disassembly would be required, but mistakes are made, and the structural design should not inhibit the fixing of said mistakes.

7.3 Flight Software

After the team received all of the data back from flight, it was realized that there were major discrepancies in the time stamps of the down-linked data. The problem occurred mainly because during flight after the team realized that something had gone wrong they tried to fix the problem by rebooting the Raspberry Pi. The problem here is that when a Raspberry Pi reboots and comes back on it checks for a time stamp, which it would usually get from a connection to wifi but during flight there is no wifi to connect to, therefore, it will take an almost random time stamp and will continue with that value. This made it difficult to accurately graph our data over time, therefore, it would be a very good idea to fly a real time clock on the payload during flight just in case something happens during flight that would require the rebooting of the Raspberry Pi.

Another problem that came up in post fight analysis were the LED's. Miura flew four LED's which were added on late in the project and only had the purpose of showing observers what was happening during testing on the ground. Consequently, it was never integrated into the code to have any sort of message down-linked that would tell the team if the LED had gone off during flight. This only became a problem during post flight testing when the team realized that the LED representing a maximum or minimum temperature was being detected for one of the components, was blinking every now and then. The team went back through the data but there was no down-link message to show whether or not the LED had been blinking during flight and therefore, they didn't know if a

temperature sensor had been tripped. Later the team knew they could go back and check for any maximum or minimum values being shown in the sensor data but it would have been useful during flight to know if these LED's were blinking or not.

Finally, there has been some discussion as to the necessity of multi-threading for future missions and whether it can be replaced with a software design that relies solely on functions. Ultimately, it was decided that although functions could provide similar organizational benefits to those provided by multi-threading, it lacks the capability of performing simultaneous operations. For example, for this mission, it was desirable for the flight software to have the ability to respond to uplink commands at any time, including while the motor was in operation. This same effect would be extremely difficult to replicate using functions alone. However, this does not exclude the possibility of using an additional form of software structure that provides similar functionality as multi-threading with greater simplicity in implementation.

7.4 Electrical and Power Systems

The basics of circuitry is mandatory to prepare for the designing and building stages of the project. With time and help from the Colorado Space Grant Consortium mentors, more information will be learned necessary to complete the mission. Learning Altium early would be advantageous. When implementing the HASP platform devices (EDAC), make sure all four ground pins are pulled together and then distributed directly to all of the payload. This will prevent ground loops from happening. Make sure that all solder connections are perfect. An 'OK' solder joint will not suffice sometimes in space conditions. Additionally, be sure to buy backup components, because items will accidentally not function due to human error. That will happen, so being prepared is necessary to be successful and to be on time with the mission schedule.

8 Moving Forward

8.1 Miura II Recommendations

Though the design flown on Miura was successful, recommendations for improvements can be made for future iterations based on the research and analysis completed during Miura. First and foremost it is recommended that any successive iterations of this mission aim to pressurize and test the payload in near space conditions. This mission did not pressurize the payload to allow for detailed structural analysis and avoid complexity for the first iteration. Pressurization is next logical stepping point in the iterative process. Pressurization is the extension method that would be used in orbit, and thus this design must be modified and tested to accommodate.

For any pressure vessel, sharp corners should be eliminated as much as possible. While this is obviously not possible for the origami layer during expansion, once expanded there should be no sharp corners on the model. Thus, the expanded design should be shifted away from a cylindrical shape and made more oblong to avoid corners where the base meets the soft material. In addition, any future design should compact in x-y direction, not just z-direction. This will increase the compactibility of the model. To this end the current wasted space in the center of compacted payload should be used more effectively.

For the next mission, multiple layers of material are essential. The payload needs to have at least one thermally insulative layer, as well as at least one pressure layer. For the pressure layer especially, multiple layers of material are recommended for redundancy. The structural layer should be made up of multiple layers of a dense weave with fine strand. It is also recommended that the seams be reinforced with a different material.

9 Acknowledgments

The team would like to thank the mentors who helped with the Miura mission, including Ross Kloetzel, Virginia Nystrom, Haleigh Flaherty, Paige Arthur, Tessa Rundle, Liz Coelho, and Brian Sanders.

They also would like to thank their sponsors; the Colorado Space Grant Consortium, the Engineering Excellence Fund, and the Undergraduate Research Opportunity Program.

References

- [1] "BEAM," *Bigelow Aerospace*, 2017, Accessed: 14 November 2017. Available: <http://bigelow aerospace.com/pages/beam/>.
- [2] Miura, K. (1985), *Method of packaging and deployment of large membranes in space*, Tech. Report 618, The Institute of Space and Astronautical Science.

A Publications

Dawson Beatty, Jacob Jeffries, Brendan Lutes, Alexandra Paquin. *Miura: Reusable Soft-Shell Structure*. Presentation and Paper, April 2017. COSGC Symposium.

Dawson Beatty, Anastasia Muszynski, Andrew Pfefer. *Miura: Reusable Soft-Shell Structure*. Presentation, November 2017. AIAA-RMS Annual Technical Symposium.

B Team Demographics

Student	Gender	Ethnicity	Race	Student Status	Disability
Nick Bearns	Male	non-Hispanic	Caucasian	Undergraduate	No
Dawson Beatty	Male	non-Hispanic	Caucasian	Undergraduate	No
Rhett Crismon	Male	non-Hispanic	Caucasian	Undergraduate	No
Adam Farmer	Male	non-Hispanic	Caucasian	Undergraduate	No
Sean Fearon	Male	non-Hispanic	Caucasian	Undergraduate	No
Jacob Jeffries	Male	non-Hispanic	Caucasian	Undergraduate	No
Courtney Kelsey	Female	non-Hispanic	Caucasian	Undergraduate	No
Brendan Lutes	Male	non-Hispanic	Caucasian	Undergraduate	No
Anastasia Muszynski	Female	non-Hispanic	Caucasian	Undergraduate	No
Alexandra Paquin	Female	non-Hispanic	Caucasian	Undergraduate	No
Andrew Pfefer	Male	non-Hispanic	Caucasian	Undergraduate	No
Mary Rahjes	Female	non-Hispanic	Caucasian	Undergraduate	No
Melanie Smith	Female	non-Hispanic	Caucasian	Undergraduate	No
Lucas Zardini	Male	Hispanic	Hispanic	Undergraduate	No
Micah Zhang	Male	non-Hispanic	Chinese	Undergraduate	No

C HASP Longitudinal Tracking

Name	Degree	Location/Current Employer
Cooper Benson	BS Aero Undergrad May 2016	Lockheed Martin
Brandon Boiko	ME Graduate BS May 2016	In Aerospace Industry
Jorge Cervantes	BS Aero 2016	MS candidate currently at CU Boulder
Becca Lidval	BS Aero May 2016	MS candidate currently at CU Boulder
Kamron Medina	Graduate may 2016	Roccor, small Aerospace company
Paige Arthur	BS Aero Undergrad May 2017	JPL
Ryan Cutter	BS Aero Undergrad May 2017	Lockheed Martin

D Requirements

High Level Requirements

- 0.1 The payload shall extend, sustain, and retract a foldable soft-shell structure multiple times.
- 0.2 The payload shall visually document the position of the soft-shell structure.
- 0.3 The payload shall numerically document the position of the soft-shell structure.
- 0.4 The payload shall numerically document the environmental conditions during flight.
- 0.5 The payload shall interface with the HASP platform.
- 0.6 The payload shall withstand an entire HASP flight.

Soft-Shell Structure Requirements

- 0.1.1 The soft shell structure shall fully extend each cycle.
- 0.1.2 The soft shell structure shall remain in its fully extended state for at least 4 minutes each cycle.
- 0.1.3 The soft shell structure shall fold into a compact form each cycle.
- 0.5.1 The soft-shell structure shall not extend past the dimensions of the payload.
- 0.6.1 The soft-shell structure shall be durable enough to last until burst.
- 0.6.1.1 The material constituting the walls of the structure shall not detach from the frame before burst.
- 0.6.1.2 The material constituting the walls of the structure shall not rip.
- 0.6.1.3 The material constituting the walls of the structure shall not have any inversions of the folded pattern that persist more than two cycles.

Image Requirements

- 0.2.1 The payload shall discern tears during each extension-contraction cycle if they occur.
- 0.2.2 The payload shall discern inversions of the folded pattern during each extension-contraction cycle if they occur.

Sensor Requirements

- 0.3.1 The payload shall measure the height of the soft-shell structure throughout each extension-contraction cycle.
- 0.4.1 The payload shall measure and record the external temperature at least once per second.
- 0.4.2 The payload shall measure and record the external pressure at least once per second.
- 0.4.3 The payload shall measure and record the acceleration of the entire payload at least once per second.
- 0.4.4 The payload shall measure and record the external humidity at least once per second.
- 0.4.5 The payload shall measure the motor's current draw at least once per second.

Interface Requirements

- 0.5.2 The payload shall not have a mass exceeding 20 kg.
- 0.5.3 The payload shall not exceed the dimensions of 38cm x 30cm x 30cm.
- 0.6.2 The payload shall remain intact and attached to the mounting plate during 10g vertical and 5g horizontal shocks.
- 0.6.2.1 The soft-shell structure shall remain securely connected to the structure for the entire duration of the flight.
- 0.6.2.2 All components shall remain securely connected to the structure for the entire duration of the flight.
- 0.6.3 The payload shall be functional at pressures of 5 to 10 mbar and lower.

Image Requirements

- 0.2.3 The entire soft-shell structure shall be visually documented during each extension-contraction cycle.
- 0.2.4 The payload shall capture visual data at night.

Data Requirements

- 0.2.5 The payload shall save the entirety of the visual data captured during the HASP flight.
- 0.2.5.1 The payload shall have enough memory to store all of the visual data captured.
- 0.3.2 The payload shall save the entirety of the positional data that is collected during the HASP flight.
- 0.3.2.1 The payload shall have enough memory to store all of the positional data collected.
- 0.4.6 The payload shall save the entirety of the environmental data that is collected during the HASP flight.
- 0.4.6.1 The payload shall have enough memory to store all of the environmental data collected.

Communication Requirements

- 0.5.4 The system shall utilize the 9-pin DB9 connector
- 0.5.4.1 The payload shall maintain communications with ground via a RS-232 serial connection.
- 0.5.4.1.1 The payload shall downlink data through a 4800 baud serial port.
- 0.5.4.1.1.1 The downlink bit rate shall not exceed 4800 bits per second.
- 0.5.4.1.1.1.1 The payload shall downlink visual data to the ground.
- 0.5.4.1.1.1.2 The payload shall downlink numerical data to the ground.
- 0.5.4.1.2 The payload shall receive 2 byte commands over the serial port.
- 0.5.4.1.2.1 The 2 byte commands shall be transmitted in hexadecimal format and execute as intended.
- 0.5.4.1.2.1.1 The payload shall be capable of receiving and executing a command to ping the payload to test communication.
- 0.5.4.1.2.1.2 The payload shall be capable of receiving and executing a command to manually adjust the height of the soft-shell structure.
- 0.5.4.1.2.1.3 The payload shall be capable of receiving and executing a command to check the status of safe mode.
- 0.5.4.1.2.1.4 The payload shall be capable of receiving and executing commands to turn safe mode on and off.
- 0.5.4.1.2.1.5 The payload shall be capable of receiving and a command to reboot the microcomputer.
- 0.5.4.1.2.1.6 The payload shall be capable of receiving and executing a command to downlink an image.
- 0.5.4.1.2.1.7 The payload shall be capable of receiving and executing a command to manually control the step count motors.
- 0.5.4.1.3 The payload shall downlink two command acknowledgements for each command uplinked to the platform.
- 0.5.4.1.3.1 The payload shall downlink an acknowledgement for each command that has been received.
- 0.5.4.1.3.2 The payload shall downlink an acknowledgement for each command that has been executed.
- 0.5.4.1.3.3 The payload shall downlink an acknowledgement for each command that fails execution.

Thermal Requirements

- 0.6.4 All electrical components shall remain within their respective stable operating temperatures.
- 0.6.4.1 All temperature sensitive components shall be thermally protected.

Power Requirements

- 0.5.5 All the components of the payload shall collectively consume no more than 75W.
- 0.5.6 The payload shall not require more than the +30 VDC provided by HASP.
- 0.5.7 The payload shall not draw more than 2.5 A.
- 0.5.8 Each component shall receive its required power.
- 0.5.9 The payload shall convert the provided VDC to the voltages necessary for operating the payload.
- 0.5.10 The power system shall utilize the provided 20 pin EDAC 516 connector.

E Code Functional Block Diagram

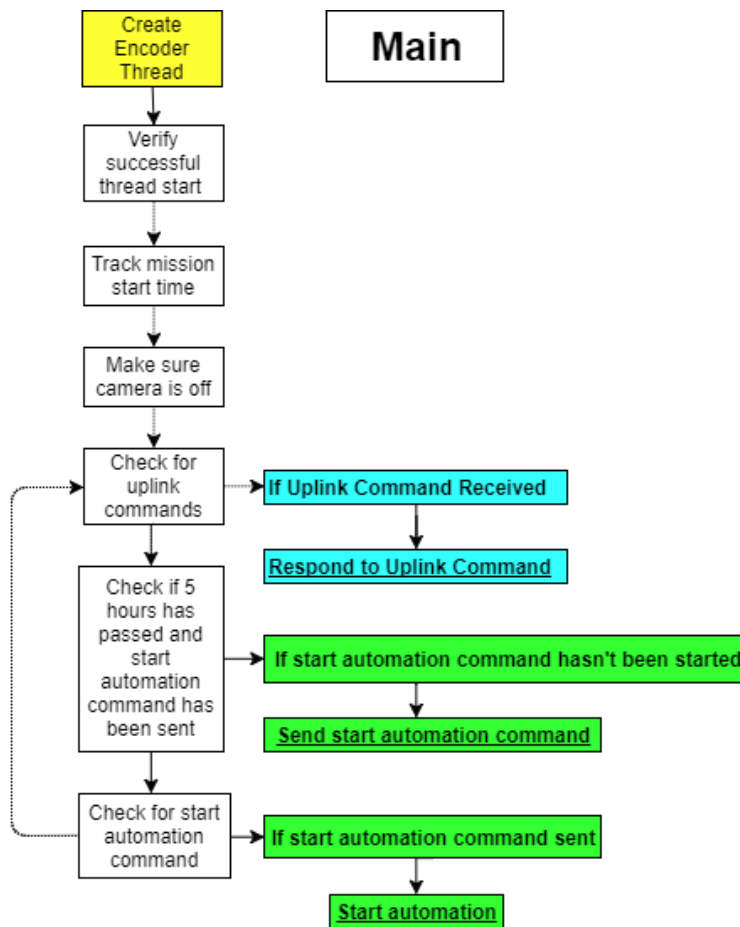


Figure 45: Main Motor Thread FBD

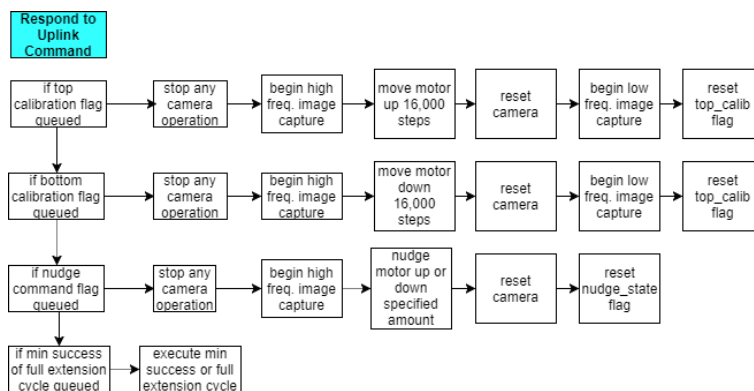


Figure 46: Camera Thread FBD

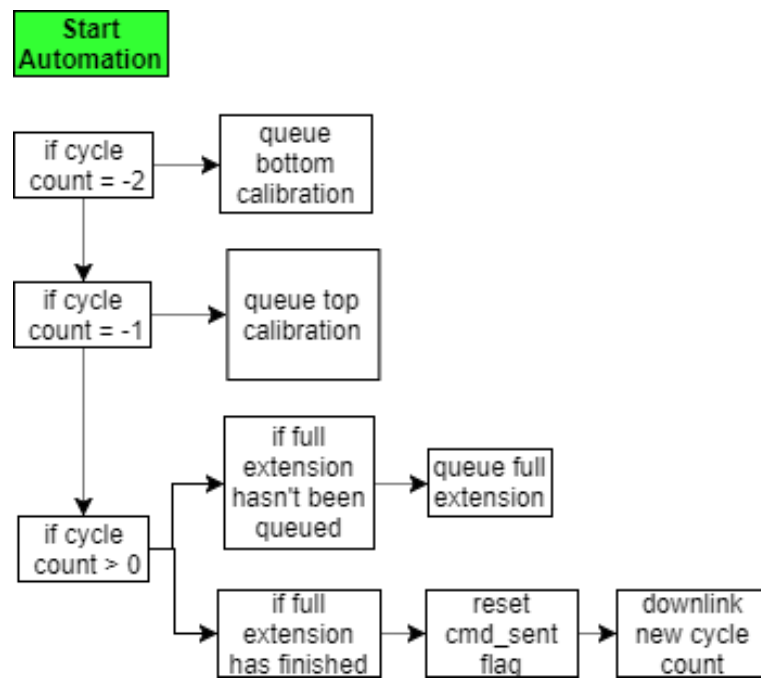


Figure 47: Camera Thread FBD

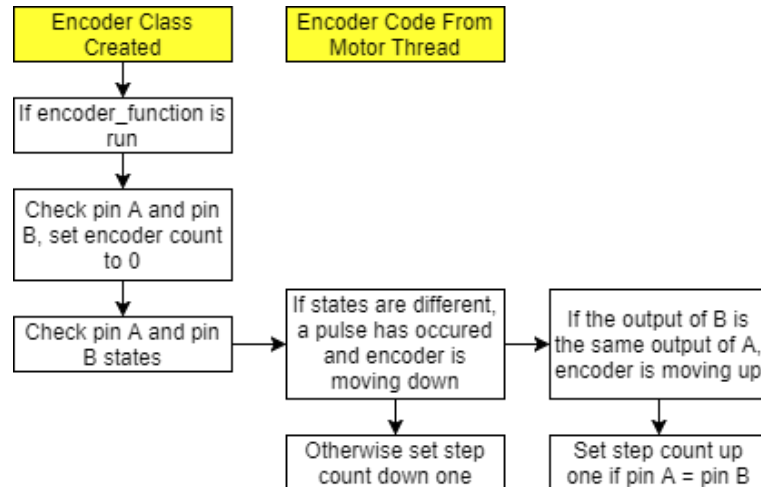


Figure 48: Encoder Thread FBD

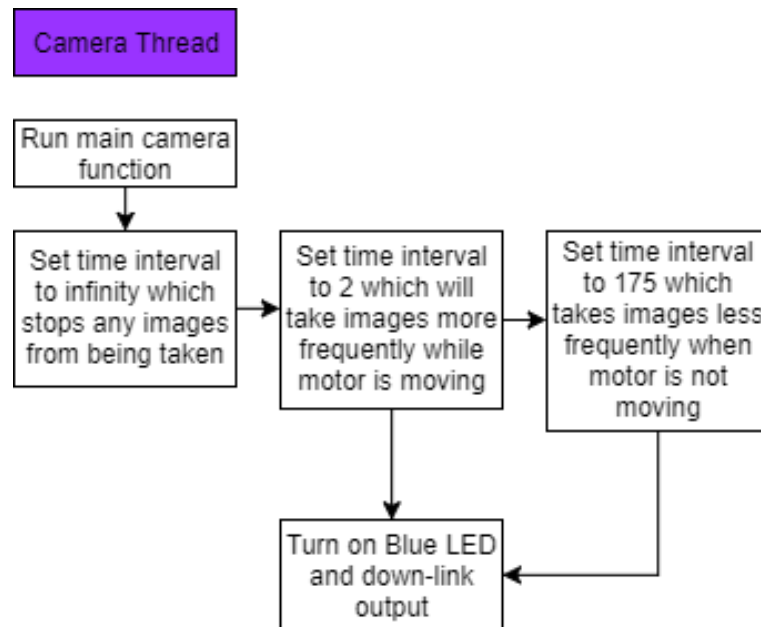


Figure 49: Camera Thread FBD